Journal of Medicinal Chemistry

pubs.acs.org/jmc Article

Modulation of the Passive Permeability of Semipeptidic Macrocycles: N- and C-Methylations Fine-Tune Conformation and Properties

Christian Comeau,[⊥] Benjamin Ries,[⊥] Thomas Stadelmann, Jacob Tremblay, Sylvain Poulet, Ulrike Fröhlich, Jérôme Côté, Pierre-Luc Boudreault, Rabeb Mouna Derbali, Philippe Sarret,* Michel Grandbois, Grégoire Leclair, Sereina Riniker,* and Éric Marsault

Cite This: *J. Med. Chem.* 2021, 64, 5365−5383 Read Online

ACCESS | Metrics & More | Article Recommendations | Supporting Information

ABSTRACT: Incorporating small modifications to peptidic macrocycles can have a major influence on their properties. For instance, N-methylation has been shown to impact permeability. A better understanding of the relationship between permeability and structure is of key importance as peptidic drugs are often associated with unfavorable pharmacokinetic profiles. Starting from a semipeptidic macrocycle backbone composed of a tripeptide tethered head-to-tail with an alkyl linker, we investigated two small changes: peptide-to-peptoid substitution and various methyl placements on the nonpeptidic linker. Implementing these changes in parallel, we created a collection of 36 compounds. Their permeability was then assessed in parallel artificial membrane permeability assay (PAMPA) and Caco-2 assays. Our results show a systematic improvement in permeability associated with one peptoid position in the cycle, while the influence of methyl substitution varies on a case-by-case basis. Using a combination of molecular dynamics simulations and NMR measurements, we offer hypotheses to explain such behavior.

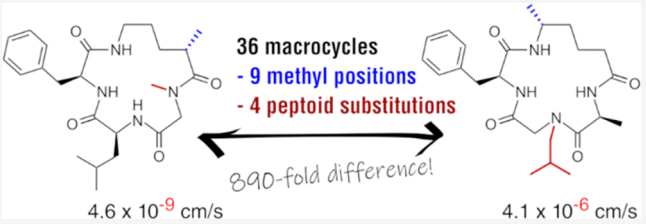

INTRODUCTION

Macrocycles have recently gathered increasing levels of interest in medicinal chemistry.[1−6] Their unique combination of conformationally constrained structure and high level of structural information allows for the design of large, organized structures suitable to interact with extended and featureless binding sites such as those found in protein−protein interactions.[7−10] Most Food and Drug Administration (FDA)-approved macrocyclic drugs belong to natural products (e.g., erythromycin, tacrolimus) or peptides (e.g., sandostatin, eptifibatin).[11] Peptidic or semipeptidic scaffolds bridge the gap between small molecules and biologics, allying synthetic ease and broad choice of natural and non-natural amino acids required for rapid and thorough pharmacophoric exploration. The main challenge with peptides resides in their physicochemical and pharmacokinetics-absorption, distribution, metabolism, and excretion (PK-ADME) properties. While cyclic peptides are typically more stable to proteases compared to their linear counterparts, their high polarity often translates into low bioavailability.[12,13] Nonetheless, some cyclic peptides cross cell membranes.[12,14,15] Developing tools and knowledge to optimize and better predict their structure−permeability relationship is therefore a requirement for the field. Such quest found inspiration in studies of the natural cyclo-undecapeptide cyclosporine A, which is administered orally. One prominent structural feature of this natural macrocycle is its high number of N-methylated residues (7 out of 11) and its dynamic structural adaptation to its environment (also known as (aka) chameleonic properties).[16−18] The effect of N-methylation on permeability of cyclic hexa- and heptapeptides has been systematically investigated since the number and position of N-methylations may be beneficial or detrimental for permeability.[15,19−23] Less explored are the N-alkylated glycines—aka peptoids—in which side chain has been moved from the α carbon to the amide nitrogen.[24] Similarly to N-methylation, this modification removes one H-bond donor, yet it also removes one stereogenic center and induces glycine-like secondary structures. The peptoid amide also facilitates cis−trans isomerization compared to the corresponding N-methylation.[25] Synthetically, the inclusion of peptoids is also compatible with solid-phase protocols and allows for an almost unlimited variety of side chains, where virtually any primary amine can be used.[26] More recently, the impact of the dynamics of macrocycles in

Received: November 23, 2020
Published: March 22, 2021

response to their environment, which can range from polar in water, nonhomogeneous in the presence of its target, to lipophilic in the membrane, has been appreciated.[17,18,27,28]

A powerful tool to modulate the properties of peptidic macrocycles is the inclusion of a nonpeptidic tether unit.[29−31] This tether can serve multiple purposes: in the context of a target interacting with a specific sequence, various tethers can be screened without modifying the peptide recognition sequence, while providing a simple handle for modulating affinity and PK properties. Small modifications in size, shape, or functional groups on the tether can dramatically influence on this kind of constrained system.[32] Additionally, a tether may facilitate macrocyclization, which can be challenging synthetically.[6] The relationship between structure and permeability is known to be elusive for this class of compounds, with small structural modifications often yielding permeability cliffs.[14,19,21,23,31,33−36]

To support our efforts in this direction[31] and pinpoint the effects of conformational modulation on permeability, we synthesized a library of closely related compounds based on chemotype **A** composed of a tripeptide tethered head-to-tail with a nonpeptidic linker (Figure 1). Two classes of

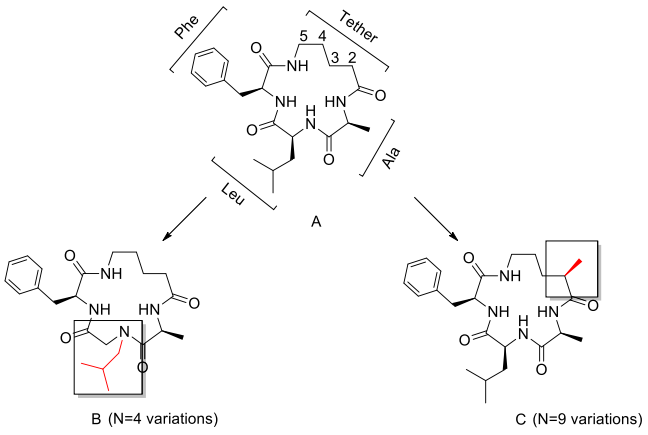

Figure 1. Two classes of modifications implemented on model compound (**A**): Nala, Nleu, and Nphe peptoids (**B** showing Nleu) and regio/stereocontrolled C-methylation (**C** showing 2*R* methylation).

modifications were implemented on chemotype **A**: single peptoid replacement (**B**, Figure 1) or regio- and stereocontrolled linker C-methylation (**C**, Figure 1). All of the possible combinations of these variations were generated, providing a total of 4 × 9 = 36 compounds with identical molecular weights (except for non-methylated tether derivatives), nearly identical sequence and identical ring sizes, leaving as little room as possible for confounding factors. The passive permeability of the resulting macrocycles was measured in the parallel artificial membrane permeability assay (PAMPA) and their cellular permeability in the Caco-2 assay.[37] We then selected two pairs of diastereomers that differ only by their stereochemistry of the tether methyl group yet either differ greatly in passive permeability or not, and performed molecular dynamics (MD) simulations coupled with solution NMR to rationalize the origin of these differences.[38]

RESULTS AND DISCUSSION

Design. The library was designed on a common sequence (Ala-Leu-Phe-Tether), with a single peptide-to-peptoid substitution and a single stereocontrolled methyl substitution on the tether (Figure 1). This created a two-dimensional array of analogs, which were named according to both the peptide and the tether substitution parameter. The symbol ⌀ on the peptide side denotes fully peptidic sequence, and on the tether side, it denotes no Me substitution. For example, compound **A** is named ⌀-⌀, **B** is termed Nleu-⌀, and compound **C** is termed ⌀-2*R*.

Chemistry. Tethers were synthesized as summarized in Scheme 1. For methyl substitution in position 2 (compound **7*S***), 5-bromovaleric acid **1** was used as the starting point. Azide substitution provided acid **2**, which was attached to Evans' oxazolidinone chiral auxiliary to provide precursor **3*S***. The latter underwent methylation to generate **4*S***, which was followed by hydrolysis to generate azidoacid **5*S*** as described by Orwig et al.[39] Azide reduction generated amino acid **6*S***, which was protected as a Boc carbamate to generate tether **7*S***. Its enantiomer **7*R*** was obtained using the other enantiomer of the chiral auxiliary. To generate 3-substituted tethers, (*R*)-citronellol **8*R*** was first oxidized to carboxylic acid **9*R***, then protected as a methyl ester **10*R***. Its double bond was then cleaved oxidatively with ozone followed by oxidative workup, yielding acid **11*R***, which was used as a substrate for Curtius rearrangement to generate Boc-protected aminoester **12*R***, which delivered Boc-protected tether **13*R*** after ester hydrolysis. Its enantiomer was generated identically from (*S*)-citronellol. On the other hand, performing the Curtius rearrangement[40] from acid **9*R*** generated Boc-protected amine **14*R***, which was oxidatively cleaved to Boc-protected tether **15*R***. Synthesis of 5-substituted tethers started from Boc-alanine **16*R*** with homologation using the Arndt−Eistert reaction,[41] followed by esterification to generate ester **18*R***, which was then reduced to the corresponding aldehyde **19*R***. The latter underwent a Horner−Wadsworth−Emmons olefination to generate unsaturated ester **20*R***. Saponification followed by double-bond hydrogenation delivered tether **22*R***. Its enantiomer was obtained from Boc-(*D*) alanine.

With the nine tethers in hand, 36 linear precursors were assembled on solid support using standard Fmoc solid-phase peptide synthesis coupled with the native tripeptide and one peptoid variation for each amino acid position (Scheme 2). Formation of the three peptoids required different methodologies: loading Nphe on resin **30** was accomplished first by loading bromoacetic acid followed by addition of benzylamine. For Nleu coupling **28**, a similar two-step methodology was used with the difference that bromoacetic acid was coupled by first activating it with *N*,*N*′-diisopropylcarbodiimide (DIC). Finally, the Nala peptoid **26** was coupled directly as it is commercially available in its Fmoc-protected form. The linear peptides were then cleaved and macrocyclized in solution as indicated in Scheme 2. Final macrocycles were purified using MS-triggered preparative high-performance liquid chromatography (HPLC) (see the Experimental Section).

Permeability Results. The passive and cellular permeabilities of the resulting library of 36 macrocycles were determined using the PAMPA and the Caco-2 monolayer assays, respectively. The latter was performed in both directions (apical-to-basolateral and basolateral-to-apical) so as to obtain a BA/AB value as a measure of efflux. The results of those experiments are summarized below (Figures 2 and 3) and available in detail in the Supporting Information (SI) (Tables S16−S18).

From the PAMPA and Caco-$2_{A\rightarrow B}$ results, it appears that: (1) the presence of a leucine peptoid (Nleu) generally increases both passive and cellular permeability significantly; (2) some

https://doi.org/10.1021/acs.jmedchem.0c02036
J. Med. Chem. 2021, 64, 5365−5383

Scheme 1. Synthesis of the Tethers[a]

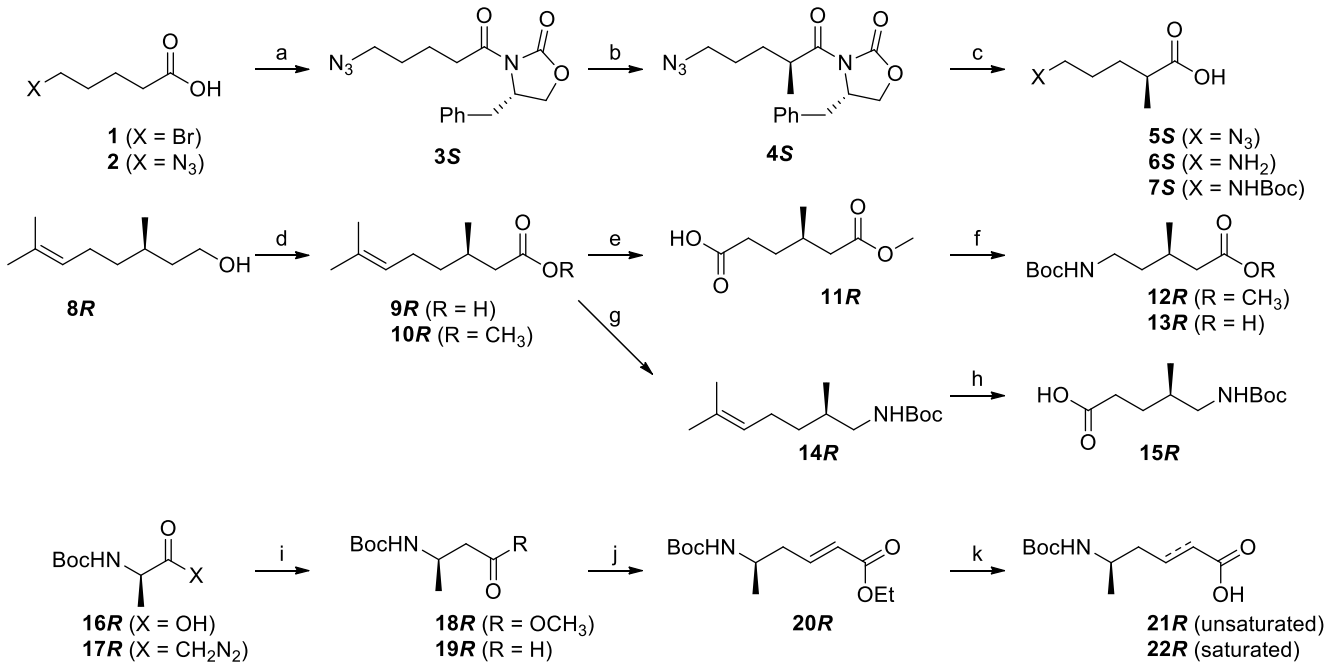

[a]Reagents and conditions: (a) (i) NaN_3, dimethyl sulfoxide (DMSO), quant.; (ii) *t*-BuCOCl, Et_3N, tetrahydrofuran (THF), 0 °C; (iii) *n*-BuLi, (*S*)-4-benzyl-2-oxazolidinone, THF, −78 °C, 81%. (b) Potassium bis(trimethylsilyl)amide (KHMDS), MeI, THF, −78 °C, 89%. (c) (i) H_2O_2, LiOH, H_2O/THF, 98%, diastereomeric excess (de): 75%; (ii) Pd/C, H_2, MeOH/AcOH; (iii) $(Boc)_2O$, $NaHCO_3$, dioxane/H_2O, 39%. (d) (i) Pyridinium dichromate (PDC), dimethylformamide (DMF), 72%; (ii) CH_2N_2, Et_2O, 95%. (e) $RuCl_3$, $NaIO_4$, CCl_4/acetonitrile (ACN)/H_2O, 70%. (f) (i) diphenylphosphoryl azide (DPPA), Et_3N, *t*-BuOH, reflux, 56%; (ii) LiOH, MeOH/H_2O, 80%. (g) Boc_2O, NaN_3, $Zn(OTf)_2$, Bu_4NBr, *t*-BuOH, THF, 33%. (h) (i) O_3, MeOH, −78 °C; (ii) H_2O_2, NaOH, H_2O, 60%. (i) (i) isobutylchloroformate, Et_3N, THF, −10 °C; (ii) CH_2N_2, Et_2O, 52%; (iii) AgOBn, Et_3N, MeOH, 70%. (j) (i) DiBAl-H, dichloromethane (DCM), −78 °C; (ii) triethyl phosphonoacetate, NaH, THF, 0 °C, 72%. (k) (i) NaOH, H_2O/MeOH, 96%; (ii) H_2, Pd/C, MeOH, 99%.

Scheme 2. Solid-Phase Synthesis[a]

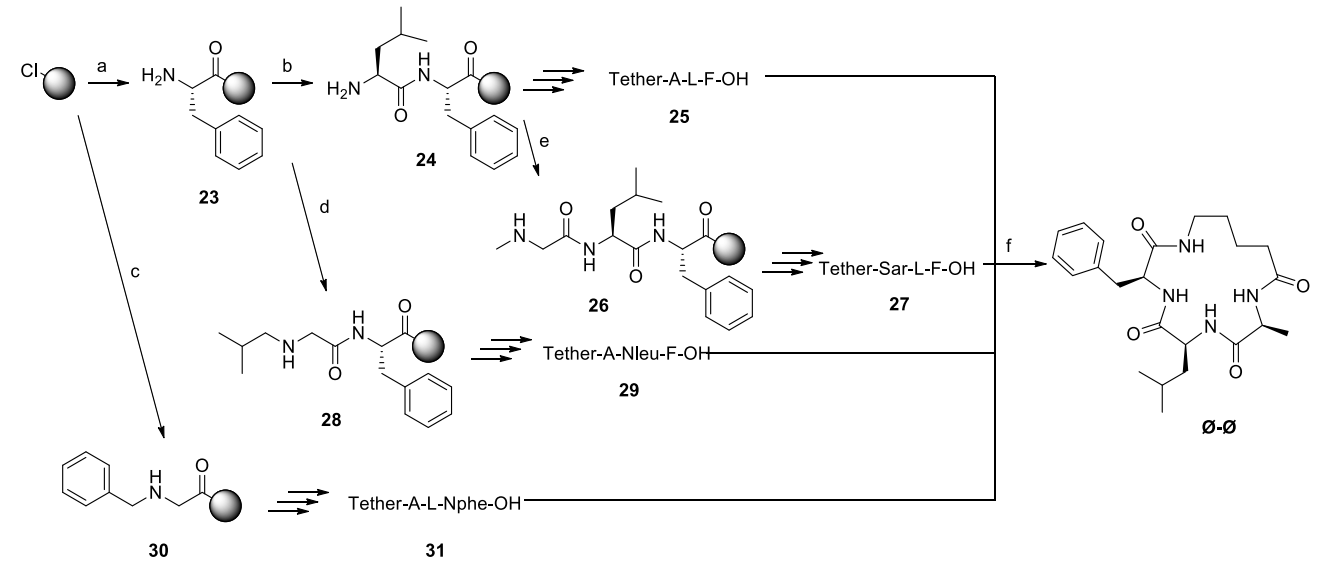

[a]Reagents and conditions (exemplified for macrocycle Ø-Ø): (a) (i) Fmoc-Phe-OH, *N*,*N*-diisopropylethylamine (DIPEA), DCM, 16 h; (ii) piperidine, DMF, 2 × 5 min; (b) (i) Fmoc-Leu-OH, 1-[bis(dimethylamino)methylene]-1*H*-1,2,3-triazolo[4,5-*b*]pyridinium 3-oxide hexafluorophosphate (HATU), DIPEA, DMF, 3 h; (ii) piperidine, DMF, 2 × 5 min; (c) (i) bromoacetic acid, DIPEA, DCM 45 min; (ii) benzylamine, DMF, 45 min; (d) (i) bromoacetic acid, DIC, DMF, 45 min; (ii) isobutylamine, DMF, 45 min (e) (i) Fmoc-Sar-OH, HATU, DIPEA, DMF, 3 h; (ii) piperidine, DMF, 2 × 5 min; (f) (i) 30% 1,1,1,3,3,3-hexafluoro-2-propanol (HFIP)/DCM, 2 × 30 min; (ii) (3-(diethoxyphosphoryloxy)-1,2,3-benzotriazin-4(3*H*)-one) (DEPBT), DIPEA, DMF, 16−72 h.

epimers possess remarkably different passive permeability values; for instance, Nleu-5R and Nleu-5S differ in passive permeability by 2 orders of magnitude yet are structurally distinct only by the orientation of the linker methyl group; and

https://doi.org/10.1021/acs.jmedchem.0c02036
J. Med. Chem. 2021, 64, 5365−5383

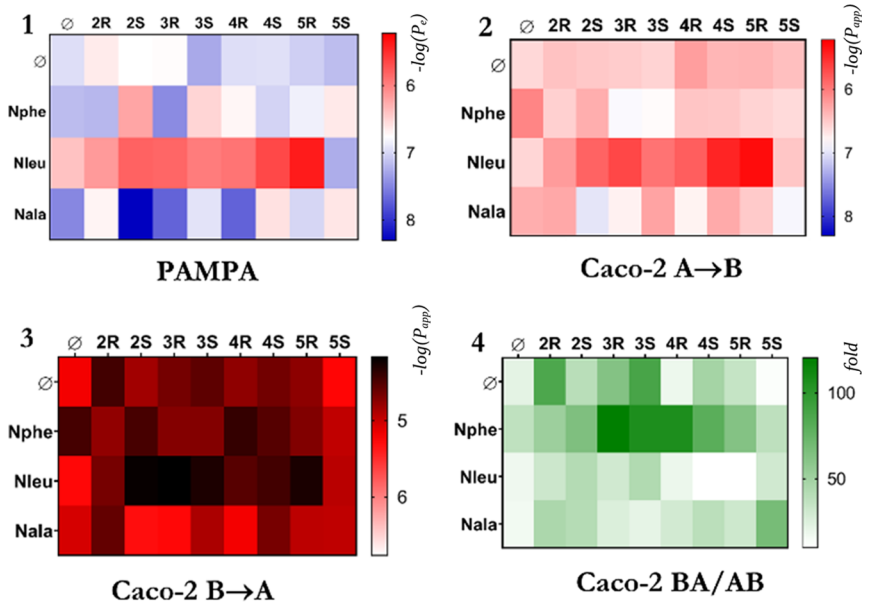

Figure 2. Permeability results in the form of heatmaps. For heatmaps 1−3, the values are expressed as $-\log(P_{app})$, so lower values mean higher permeability (in order of increasing permeability: blue, white, red, and black). Heatmap 4 shows the BA/AB ratio, which represents a measure of efflux.

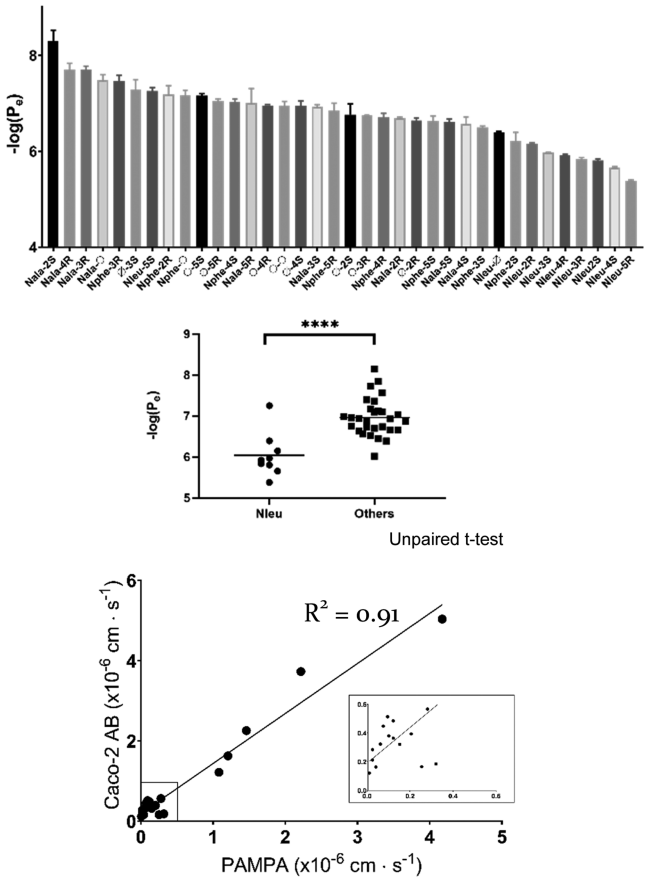

Figure 3. (Top) PAMPA results with standard deviation, ranked; (middle) statistical analysis of the PAMPA data shows a significant ($p < 0.0001$; unpaired *t*-test) effect for the Nleu vs other macrocycles; and (bottom) a good correlation between PAMPA and Caco-$2_{A\rightarrow B}$ ($R^2 = 0.91$).

(3) compared to the reference macrocycle ø-ø, some modifications are detrimental to both passive and cellular permeabilities, while others are favorable.

From the basolateral to apical (Caco-$2_{B\rightarrow A}$) results, we calculated the BA/AB ratio as a measure of efflux.[42] Values range from 10 to 120, which leaves no doubt that this class of compounds is generally subject to efflux. It is, however, interesting to observe that the Nleu peptoid series also stands out in the Caco-2 assay in both directions, suggesting that passive permeability is the main differentiating factor for this series of compounds, not efflux. There is in fact a good correlation ($R^2 = 0.91$) between PAMPA and Caco-$2_{A\rightarrow B}$ permeabilities (Figure 3). This is very different from a series of similar macrocycles published recently by our group, which bear a secondary amine instead of the third amide bond, and which showed very small PAMPA permeability distribution yet very important, SAR-able variations in Caco-2 permeability.[31]

To explain the high permeability observed with compounds containing Nleu, two hypotheses can be invoked: (A) the Nleu peptoid is intrinsically advantageous compared to leucine; or (B) position 2 in the ring benefits most from peptoid substitution. To answer this question, we inverted the positions of Ala and Leu in the sequence and tried both substitutions (Figure 4). PAMPA permeability supports hypothesis B: the permeability-enhancing effect observed in the Nleu series is due to the N-alkylation at position 2.

There are a few differences between an amino acid and its peptoid. Namely, the peptoid has (1) no H-bond donor; (2) a

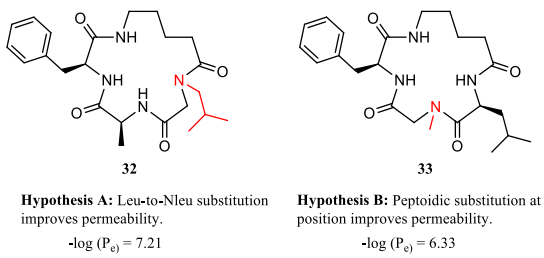

Figure 4. Inverting peptoid positions to better understand whether higher permeabilities observed with Nleu are due to its nature or to its position within the macrocycle.

https://doi.org/10.1021/acs.jmedchem.0c02036
J. Med. Chem. 2021, 64, 5365−5383

slightly stronger H-bond acceptor due to the higher substitution on the nitrogen atom; (3) a lower cis/trans transition barrier; (4) higher backbone flexibility due to the absence of a chiral side chain on the α carbon; and (5) no chirality. We designed additional compounds based on the original Ala-Leu-Phe-tether scaffold to untangle some of those effects and pinpoint the most permeability-enhancing modification introduced by this peptoid substitution (Figure 5). The 2S linker was chosen for those additional compounds because this series shows the most statistically significant differences among themselves in PAMPA (Figure 2).

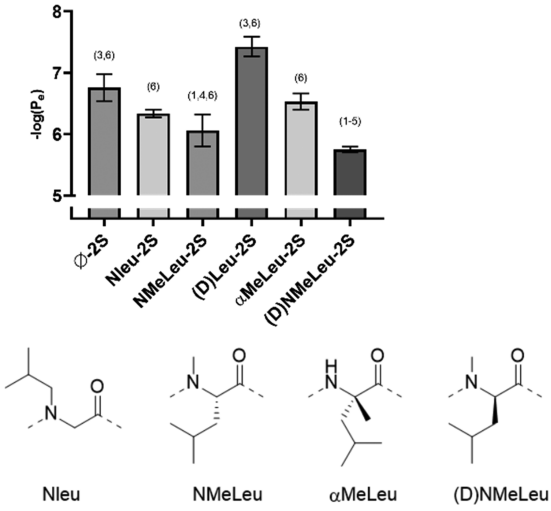

Figure 5. Four additional compounds to better elucidate the reason why a peptoid in this position has a beneficial effect on passive permeability. All leucine derivatives are in position 2. Numbers in parentheses indicate a significant difference ($p < 0.05$; one-way analysis of variance (ANOVA)/Tukey).

Two compounds appear more permeable than Nleu-2S: NMeLeu-2S and (D)NMeLeu-2S, suggesting that substituting the amide proton is beneficial. Indeed, both (D)Leu-2S and αMe-Leu-2S, which still have this amide proton, display a lower permeability than Nleu-2S. From the point of view of identifying why Nleu was found to be so successful, we can also rule out the orientation of the side chain: the three most permeable compounds are (D)NMeLeu-2S, NMeLeu-2S, and Nleu-2S and thus all orientation are represented. Two other factors could explain why (D)NMeLeu-2S and NMeLeu-2S show higher permeability than Nleu-2S (other than the slight increase in lipophilicity associated with an additional methyl group, an effect shared with the poorly permeable αMe-Leu-2S): they possess lower backbone flexibility, losing the glycine-like effect of peptoids, and they would be expected to have a smaller cis population as the methyl is less bulky than the isobutyl chain.[25,43,44] However, these effects do not seem to be as important as the loss of the H-bond donor (compare αMe-Leu-2S with Nleu-2S), and do not hold comparison with ø-2S, which also has reduced backbone flexibility and lower expected cis population. In summary, the strongest factor appears to be the loss of the H-bond donor. The increased permeability observed with the Leu-to-Nleu substitution therefore appears to be caused by a change in the intramolecular H-bonding pattern. While it is likely that this pattern also explains why the peptoid substitution was successful at this position and not for Nala and Nphe, we did not investigate this sequence-dependent point further.

As for the influence of the methyl group, no obvious trend could be observed. Yet, there are some significant differences between pairs of epimers. Also, the sole exception to the increase in permeability with Nleu was found in compound Nleu-5S, while its epimer Nleu-5R is the most permeable of the series. We decided to investigate this central observation by analyzing the associated conformations in greater detail using a combination of structural data (NMR measurements) and computer-simulated trajectories (molecular dynamics simulations).

A "permeability cliff" such as that observed between Nleu-5R and Nleu-5S (Figure 6) is also observed, to a lesser extent,

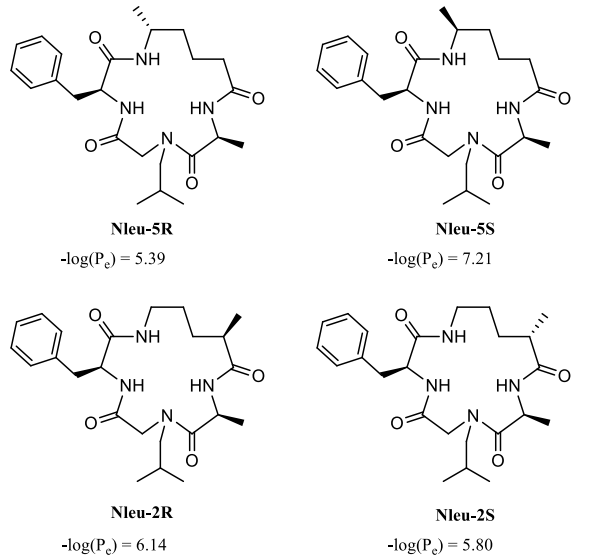

Figure 6. Selected cyclic peptides studied with experimental NMR analysis and molecular dynamics (MD) simulations.

between some other pairs of epimers (e.g., Nala-4R vs 4S with $-\log(P_e)$ = 7.63 and 6.63, Nphe-2R vs 2S with 7.16 and 6.31, and Nphe-3R vs 3S with 7.49 and 6.49). To obtain a better understanding of the underlying conformational changes, extensive MD simulations of the Nleu-5R and Nleu-5S macrocycles (the most distant epimers in terms of permeability) were performed in both polar and apolar environments (i.e., water and chloroform). The starting conformations used for simulations showed similar distributions in terms of hydrogen bonds (H-bonds) and backbone torsional angles (Tables S7 and S8 in the SI). For each molecule, approximately 50% of the starting structures had a *trans*-peptoid bond and 50% had a *cis*-peptoid bond. As a control, we used a second pair of peptides (Nleu-2S and Nleu-2R) with the same structural change but similar PAMPA permeability (see Table S16 in the SI).

The cumulative 25 μs simulation data for each peptide and solvent were clustered separately based on the backbone dihedrals and the polar atom distances. The resulting clusters could be structurally classified depending on the conformation of the peptoid bond (i.e., cis or trans; see Tables S9 and S10 in the SI). The cis−trans isomerization represents a very slow process in the simulations, which occurred only rarely (Table S11 in the SI). Due to the low number of transitions, the process could not be modeled robustly. Therefore, the clusters with the *cis*- and *trans*-peptoid bond are analyzed separately in the following.

The NMR experiments in chloroform-*d* showed that the four compounds adopt at least two different conformations in

https://doi.org/10.1021/acs.jmedchem.0c02036
J. Med. Chem. 2021, 64, 5365−5383

solution. The major conformer was identified with all amides in trans conformation (Table S1 in the SI). It was not possible to assign the minor conformers due to signal overlap and low intensity. In the case of Nleu-5R and Nleu-5S, a third conformer could be identified based on exchange spectroscopy (EXSY) cross-peaks in the nuclear Overhauser enhancement spectroscopy (NOESY) spectrum, which is barely detectable in the ^{1}H spectrum. The corresponding conformer ratios are listed in Table 1. The results from the MD simulations are compared to

Table 1. Ratios of Conformer Population Observed in NMR Spectra ($CDCl_3$)

compound	ratio
Nleu-2R	100:8
Nleu-2S	100:3
Nleu-5R	100:4:0
Nleu-5S	100:16:1

the NMR data of the major conformer (i.e., $^3J_{HN-H\alpha}$ coupling constants and nuclear Overhauser effect (NOE)-derived distances, given in Tables S2−S6 in the SI) to validate the simulation results.

The clusters with all amides in trans conformation are in good agreement with the $^3J_{HN-H\alpha}$ coupling constants (Figure 7), whereas the clusters containing the *cis*-peptoid bond deviate significantly from the experimental values. For Nleu-2R, the $^3J_{HN-H\alpha}$ coupling analysis is missing as we could not determine the $^3J_{HN-H\alpha}$ couplings reliably due to line broadening in the spectrum. The NOE upper distance bounds are also generally reproduced in these clusters (Figures S5−S9 in the SI). Based on these findings, we focus the analysis in the following on those clusters, which have a reasonable agreement with the NMR data (i.e., clusters 1 and 4 for Nleu-5R, clusters 1, 5, and 6 for Nleu-5S, cluster 1 for Nleu-2R, and clusters 1 and 2 for Nleu-2S).

A necessary condition for good membrane permeability is the adoption of conformations that shield polar groups optimally from the apolar environment.[45−47] Therefore, we first analyzed the hydrogen-bonding patterns in the clusters in chloroform. For the peptides in this study, a maximum number of two H-bonds can be formed in a conformation due to ring strain. As can be seen in Table 2, the percentage of sampled conformations

Table 2. Percentage of Sampled Conformations with Zero, One, or Two Hydrogen Bonds in Chloroform[a]

number of hydrogen bonds	0	1	2
Nleu-5R (%)	8	63	30
Nleu-5S (%)	25	68	7
Nleu-2R (%)	15	64	21
Nleu-2S (%)	13	74	13

[a]Analysis was restricted to the clusters with the *trans*-peptoid bond.

with two H-bonds differs significantly between Nleu-5R (30%) and Nleu-5S (7%). At the same time, the percentage of conformations without a H-bond is increased for Nleu-5S (25%) compared to Nleu-5R (8%). For the other pair, Nleu-2R and Nleu-2S, the percentages are more similar and in between those of Nleu-5R and Nleu-5S.

For a given molecule in an apolar environment, having access to conformations in which polar groups are shielded—such as by H-bonding—should be energetically favorable. To assess this effect, we extracted the potential energy of the peptides (i.e., intramolecular and peptide-solvent contributions) from the trajectories. The normality of each potential-energy distribution was confirmed by the Shapiro−Wilk test[48] (Table S12 in the SI). The Fisher *t*-test[49] was employed to determine if the means of the distributions differ statistically significantly ($p < 0.05$). This was found to be the case for each pair of distributions (Table S13 in the SI). On average, the potential energy of Nleu-5R is 9 kJ/mol lower (i.e., more favorable) in chloroform compared to Nleu-5S, whereas the difference in the average potential energy between Nleu-2R and Nleu-2S is 6 kJ/mol. In many studies in the literature, it was found that the three-dimensional (3D) polar surface area (3D-PSA) is a good measure for the degree of polar shielding in conformations.[31,45,50,51] However, for the present set of four peptides, no correlation was observed between the 3D-PSA and the potential energy (Figure S10 in the SI). The ring strain in the relatively small backbone cycle of the peptides affects the geometry of the intramolecular H-bonds,

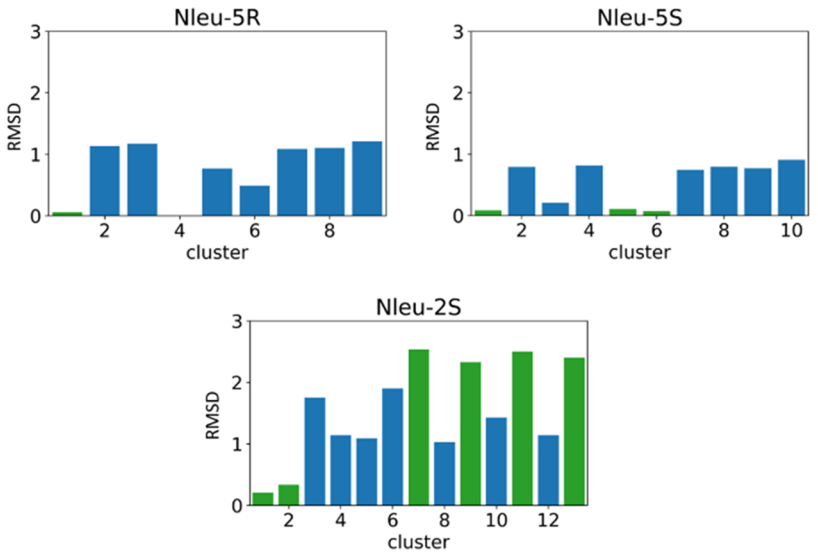

Figure 7. Root-mean-square deviation (RMSD, in hertz) between $^3J_{HN-H\alpha}$ coupling constants in chloroform from NMR measurements and from MD simulations. Clusters with the peptoid bond in trans conformation are shown in green.

https://doi.org/10.1021/acs.jmedchem.0c02036
J. Med. Chem. 2021, 64, 5365−5383

which is likely not reflected appropriately in the 3D-PSA calculation. In summary, the ranking Nleu-5R < Nleu-2S < Nleu-2R < Nleu-5S, which was found in terms of both hydrogen-bonding patterns and potential energies, matches well with the experimental permeability data.

The findings described above indicate that the change in stereochemistry of the methyl group in position 5 between Nleu-5R and Nleu-5S leads to different conformational behavior. A detailed analysis of the H-bonds showed that only Nleu-5S forms a H-bond between Ala-O and the tether-NH with an occurrence of 24% in chloroform (Table 3). This H-bond across the ring of Nleu-5S prevents the formation of other H-bonds (Figure 8B). Such a conformation with a single H-bond is likely less favorable (compared to one with more H-bonds) in chloroform because less polar groups are shielded. In the dominant conformation of Nleu-5R, on the other hand, two H-bonds can be formed across the ring (Figure 8A).

Table 3. Hydrogen Bond Occurrence in Percentage for the Sampled Conformations in Chloroform[a]

H-bond	Nleu-2R (%)	Nleu-2S (%)	Nleu-5R (%)	Nleu-5S (%)
Nleu-O tether-NH	74	37	28	33
Ala-O tether-NH	<1	<1	<1	24
Phe-O Ala-NH	<1	35	57	<1
Ala-O Phe-NH	27	25	36	17

[a]Analysis was restricted to the clusters with the *trans*-peptoid bond.

Next, we analyzed the torsional-angle distributions in the backbone ring of the peptides. The change in stereochemistry of the methyl group at position 5 leads to a shift in the torsional-angle distributions of the tether units for Nleu-5S compared to Nleu-5R (Figure 9A). This shift results in a bent conformation of the ring (Figure 9B), which allows only one H-bond to form between Ala-O and tether-NH (Figure 10). There is also a shift in the backbone torsional-angle distributions between Nleu-2R and Nleu-2S, however, to a much smaller extent (Figure S11 in the SI).

The results for the simulations in water are given in the SI (Tables S10−S15). The analysis of the hydrogen-bonding patterns in water showed that Nleu-5R has a higher percentage (about 10%) of conformers with no H-bonds compared to Nleu-2R, Nleu-2S, and Nleu-5S (Table S14). In general, however, no major differences between the peptides could be observed in water.

The findings, taken together, suggest that the permeability cliff observed between Nleu-5R and Nleu-5S is related to their propensity for conformations with a maximized number of intramolecular H-bonds in the apolar environment. Their ability to adopt such conformations is in turn affected by the stereochemistry of the methyl group at position 5 in the tether as it determines the preferred torsional angles of the tether.

CONCLUSIONS

A total of 42 macrocycles were synthesized and their permeability assessed in the PAMPA and Caco-2 assays. The combination of these data, NMR measurements, and molecular dynamics simulations allows us to draw some conclusions that are hopefully applicable to other systems. The systematic higher permeability of macrocycles bearing an Nleu peptoid is striking and well above statistical significance. Our experiments suggest this effect is due to the removal of this specific H-bond donor, thus working similarly to the more widely used N-methylation strategy. This systematic effect shows that "masking" H-bond donors should be considered early in the design of cyclic peptides. Possibly, it is a matter of finding the right one(s), i.e., those that allow for the most favorable H-bonding patterns in the rest of the macrocycle.

The methyl position on the tether had little effect in most cases, with a few notable exceptions. Nala-2S has the lowest passive permeability, while its epimer is average. Conversely, Nleu-5R is the most permeable compound from our initial library, while its counterpart Nleu-5S is the exception among the Nleu compounds for its low permeability. A detailed analysis of torsion angles points once more at intramolecular H-bonds. Nleu-5R and Nleu-5S have different intramolecular H-bonding patterns. It seems likely that the 2 and 5 positions have the highest potential to introduce significant conformational changes due to their proximity to H-bond partners (the tether's carbonyl and nitrogen, respectively). These positions might also have more impact due to the flexible nature of the tether we used, as they are close to the sp^2-like amides. It is also noteworthy that a simple inversion of stereochemistry was shown to exert long-distance influence, modifying the phenylalanine's rotation.

Altogether, this study sheds light on the relationship between structure and permeability in this class of compounds. The two seemingly very different substitutions we explored were both found to affect permeability through a change in the intramolecular H-bonding pattern.

EXPERIMENTAL SECTION

PAMPA.[53,54] Passive permeability assays were run in triplicate on 96-well hydrophobic poly(vinylidene difluoride) (PVDF) plates (Millipore, 0.45 μM, 200 μL) and 300 μL receptor plates (Millipore).

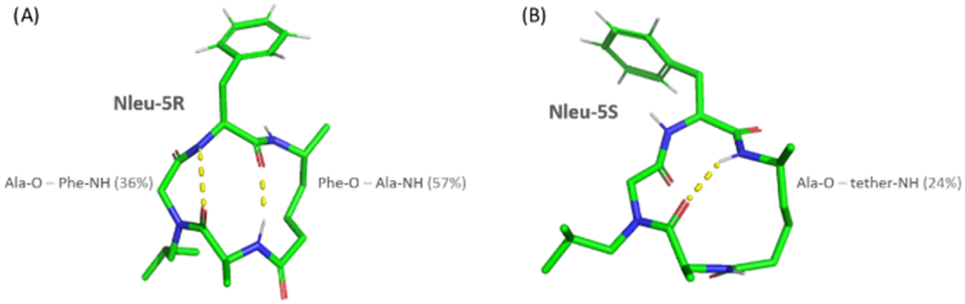

Figure 8. Snapshots of Nleu-5R (A) and Nleu-5S (B) from MD simulations in chloroform. Hydrogen bonds are shown with their percentage of the absolute occurrence in chloroform in the *trans*-peptoid clusters. Pictures were generated with PyMol.[52]

https://doi.org/10.1021/acs.jmedchem.0c02036
J. Med. Chem. 2021, 64, 5365−5383

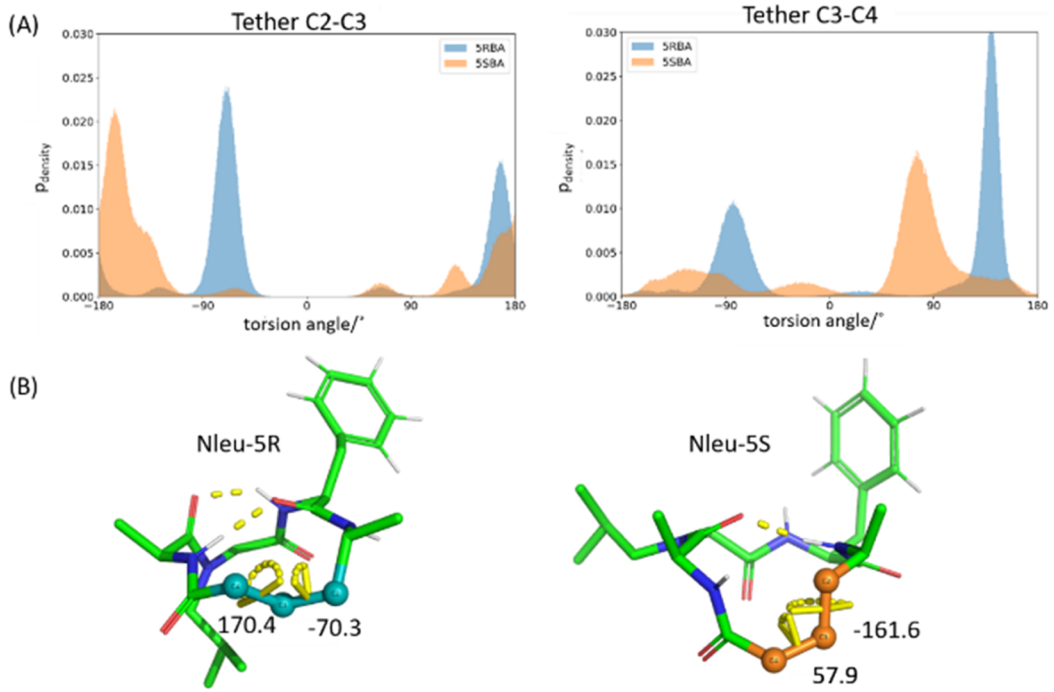

Figure 9. (A) Torsional-angle distributions of the tether in Nleu-5R (blue) and Nleu-5S (orange) in chloroform. The analysis was restricted to the clusters with the *trans*-peptoid bond. (B) Torsional angles of the tether (shown in cyan and orange) corresponding to the peaks of the distributions. Pictures were generated with PyMol.[52] The change in the stereocenter also affects the χ_1-angle of the phenylalanine residue as the tether conformation hinders the rotation around this torsion due to a steric clash with the carbonyl group that is facing out of the backbone ring (Figure 10).

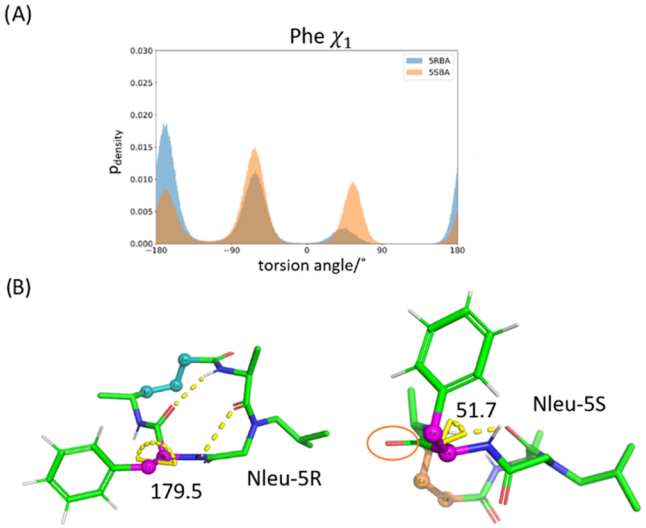

Figure 10. (A) Torsional-angle distributions of the χ_1 torsional angle of the phenylalanine residue in Nleu-5R (blue) and Nleu-5S (orange) in chloroform. Analysis was restricted to the clusters with the *trans*-peptoid bond. (B) χ_1 torsional angle of the phenylalanine residue (shown in purple) corresponding to the peaks of the distributions. The backbone carbonyl interferes with the rotation around this torsion is highlighted with a red circle. Pictures were generated with PyMol.[52]

Assays were carried out using a 10 μL membrane (2% lecithin in dodecane) with a 100 μM solution in a phosphate buffer (pH = 6.4) and shaken for 17 h (25 °C, 50 rpm).

Caco-2 Assay.[54−56] Assays were run in triplicate on polycarbonate Transwell plates (Corning) with hydrophilic filters (0.45 μM, Millipore). Caco-2 cells were passaged >72 times and grown on the filter for 22 days, at which point the transepithelial electrical resistance (TEER) was over 300 Ω cm^2. Compounds were tested in an initial 10 μM solution using an Hank's balanced salt solution (HBSS) buffer (*N*-(2-hydroxyethyl)piperazine-*N*′-ethanesulfonic acid (HEPES)/NaOH, pH = 7.4) and a sample was taken after 60 and 120 min at 37 °C. Propranolol and atenolol were used as control compounds for high and low permeabilities, respectively. The assays were performed in both apical-to-basolateral and basolateral-to-apical directions to better assess the effect of efflux.

Simulation. In the computational studies, two pairs of structurally similar cyclic peptides were selected, i.e., Nleu-5R/Nleu-5S and Nleu-2R/Nleu-2S. The first pair presents a "permeability cliff", i.e., the two peptides show a large difference in the passive permeability in the PAMPA assay (Nleu-5R: 5.39; Nleu-5S: 7.21), despite a high structural similarity. In contrast, the second pair is similar in both structure and permeability (Nleu-2R: 6.14; Nleu-2S: 5.80). For each of these four peptides, 250 starting coordinates were generated using the macrocycle variant of the OMEGA conformer generator from OpenEye.[57−59] Conformers were energy-minimized for maximum 2000 steps with the steepest descent[60] approach using the GROMOS software package[61] with the GROMOS 54A7 force field.[62] Each minimized starting conformation was solvated in a cubic box of simple-point-charge (SPC) water[63] (on average, 4172 solvent molecules) or chloroform[64] (on average, 980 solvent molecules). For each system, a molecular dynamics (MD) simulation of 101 ns length was performed under isothermal−isobaric (NPT) conditions with the leap-frog integration algorithm[65] and a time step of 2 fs. The first 1 ns was discarded as equilibration. Bond lengths were constrained with SHAKE[66] and a tolerance of 10^{-4} nm. Nonbonded interactions were calculated using a twin-range scheme with a short-range cutoff of 0.8 nm and a long-range cutoff of 1.4 nm. The electrostatic nonbonded contributions beyond the long-range cutoff were calculated with the reaction-field[67] approach, setting the dielectric permittivity to 61[68] for water, and to 4.8[64] for chloroform. The temperature was kept constant at 300 K using the weak coupling scheme[69] and a coupling time of 0.1 ps^{-1}. The pressure was kept at 1.031 bar (1 atm) with the same type of algorithm, a coupling time of 0.5 ps^{-1}, and an isothermal compressibility of 0.001654 bar^{-1} for chloroform and 0.0004575 bar^{-1} for water. Translational motion of the center of mass of the simulation box was removed every 2 ps. Energies and coordinates were written every 5 ps.

https://doi.org/10.1021/acs.jmedchem.0c02036
J. Med. Chem. 2021, 64, 5365−5383

Trajectory analysis was performed with PyEmma[70] and MDTraj.[71] The selection of features for the clustering consisted of the distances between all pairs of polar atoms and the backbone torsional angles, which resulted in 57 features. This selection was reduced to three to five dimensions (depending on the peptide) with TICA[72] using a cumulative variance of 0.9 as criterium and a TICA correlation lag time of 50 ps. Based on these TICs, the frames were clustered with a common nearest neighbor (CNN) algorithm[73,74] using a cutoff of 0.2 and a similarity of 20. Comparison of selected clusters with NMR experiments was performed with the GROMOS++ package of programs.[75] The coefficients for the Karplus curve were taken from Vögeli et al.[76] Analysis of hydrogen bonds and torsional angles was performed with MDTraj. The 3D polar surface area (3D-PSA) was calculated with our implementation[28] of the workflow in ref 47 using PyMol.[52] Statistical analysis of all results was carried out using the Python packages pandas, NumPy and SciPy.[77]

NMR Measurements. The selected peptides Nleu-5R, Nleu-5S, Nleu-2R, and Nleu-2S were characterized by NMR in chloroform-*d* (Cambridge Isotope Laboratories). The following spectra were recorded if not stated otherwise: ^{1}H NMR, total correlation spectroscopy (TOCSY), double-quantum filtered correlation spectroscopy (COSY), multiplicity edited ^{13}C heteronuclear single quantum coherence (HSQC), ^{13}C heteronuclear multiple bond correlation (HMBC), and NOESY. All spectra were measured at 25 °C on a Bruker Avance III HD 600 MHz spectrometer equipped with a N_2-cooled Prodigy triple resonance probe. ^{13}C HSQC and TOCSY spectra were recorded with sensitivity enhancement. TOCSY was run with an 80 ms DIPSI2 isotropic mixing time. The mixing time for the NOESY experiments was set to 300 ms if not stated otherwise. For compound Nleu-5R, an EASY-ROESY[78] spectrum with 100 ms mixing time was recorded instead of a NOESY. For all spectra, the time domain in both dimensions was extended to twice its size by zero filling, apodized with a $\cos^2$ function, and the baseline of the resulting spectra was corrected with a polynomial of fifth order or using the Whittacker smoother algorithm.[79] Processing was done with Bruker TopSpin version 4.0 (Bruker Biospin AG) and MestReNova 12.0 (Mestrelab Research). Resonance assignment and volume integration of the ROESY cross-peaks were performed with SPARKY 3.115.[80] The assignments are summarized in Table S1 in the SI.

$^{3}J_{\mathrm{HN-H}\alpha}$ coupling constants for compounds Nleu-5R, Nleu-5S, Nleu-2R, and Nleu-2S were extracted directly from the ^{1}H spectrum with MestReNova and are summarized in Table S2 in the SI.

Volumes were extracted from NOESY and ROESY spectra by integration of the cross-peaks with a Gaussian function (eq 1).

$$r_{1,2} = a + b \times V_{1,2}^{-(1/6)} \quad (1)$$

$V_{1,2}$ is the volume of the cross-peak between proton 1 and 2, a and b are fitting parameters, and $r_{1,2}$ is the corresponding interatomic distance. A two-point calibration was done with the averaged interatomic distance (e.g., on both sides of the diagonal) between the diastereotopic protons NLeu Hα_1−Hα_2 (1.8 Å) and the distance between Hα and Hβ* in the alanine residue (2.65 Å).[81] In the second case, the volume was previously divided by 3 to account for the three protons in the methyl group. Cross-peaks integrated on both sides of the diagonal were averaged, and error bonds of ±20% were added to the calculated distance. Since the GROMOS++ programs can do multiplicity correction and averaging over indistinguishable protons automatically, the reported data do not account for that. The volumes and the corresponding distances can be found in Tables S3−S6 in the SI.

Materials and Equipment Used in Synthesis. All solvents and chemicals were used as purchased without further purification. The progress of all reactions was monitored on Silicycle silica gel plates using either ethyl acetate/*n*-hexane or dichloromethane/methanol. Column chromatography was performed with SILIFLASH P60 silica (40−63 μM, 230−400 mesh, 60 Å).

NMR data were recorded on a Bruker Ascent 400. Chemical shifts are given in parts per million (ppm) (δ relative to the residual solvent peaks for both ^{1}H and ^{13}C). Chloroform (7.27 ppm), DMSO (2.50 ppm), and MeOH (3.31 ppm) were used as the internal standards for protons and for carbons (77.0, 39.5, and 49.2 ppm, respectively).

High-resolution mass spectrometry (HRMS) was performed with a maXis (electrospray ionization quadrupole time-of-flight (ESI-QTOF)).

Final products were purified on a Waters preparative HPLC system (Waters Sample Manager 2767, Binary Gradient Module 2545, SQ Detector 2) with an XSelect Peptide CSH C18 OBD Prep Column (100 × 19 mm^2, 5 μM spherical particle size) with a flow of 20 mL/min on a 15 min gradient of varying proportions of acetonitrile in water containing 0.1% formic acid (in both solvents).

Purity analysis of the final macrocycles was performed with UPLC/MS Acquity H-Class using a BEH C18 column (50 × 2.1 mm^2, 1.7 μM spherical particle size) with a flow of 0.8 mL/min on a 2.5 min gradient from 5 to 95% acetonitrile in water containing 0.1% formic acid (in both solvents). All chromatography equipment was purchased at Waters (Canada). The purity was determined from the UV spectrum, by the ratio of the area under the curve (AUC) of the expected compound over the sum of the AUC of all peaks that did not also appear on blanks. All final macrocycles were obtained with a purity of >95%.

Loading and Capping Procedure 23. To Wang resin (200 mg, nominal loading: 1.5 mmol/g) was added anhydrous THF (2 mL), and the mixture was left for 30 min. Meanwhile, a solution of Fmoc-Phe-OH (3 equiv) was prepared in anh. THF (2 mL). To this solution was added PPh_3 (3 equiv) and diisopropyl azodicarboxylate (DIAD) (3 equiv). The THF from the resin solution was removed by filtration, and the amino acid solution was added. The mixture was left on an orbital shaker overnight. The resin was then filtered and washed in the following sequence: 3× DMF, 3× DMC, 3× *i*PrOH, 3× DCM, 3× *i*PrOH, 3× DCM. A freshly prepared solution of DCM/Ac_2O/DIPEA (15:2:1, 2 mL) was then added, and the mixture was left on an orbital shaker for 30 min, after which it was washed using the same sequence as above.

Loading Procedure for Nphe 30. To a 2-chlorotrityl chloride resin (200 mg, nominal loading: 1.2 mmol/g) was added anhydrous DCM (2 mL), and the mixture was left for 30 min. Meanwhile, a solution of bromoacetic acid (4 equiv) was prepared in anh. DCM (2 mL). To this solution was added DIPEA (8 equiv) The DCM from the resin solution was removed by filtration, and the bromoacetic acid solution was added. The mixture was left on an orbital shaker for 1 h. The resin was then filtered and washed six times with DMF. A solution of benzylamine (20 equiv) in DMF (2 mL) was added, and the mixture was left on an orbital shaker for 1 h. The resin was then filtered and washed six times with DMF.

Deprotection Procedure. To the resin (200 mg) was added a solution of 20% piperidine in DMF (2 mL), and the mixture was left on an orbital shaker for 20 min. The resin was then washed twice with DMF, and a solution of 20% piperidine in DMF (2 mL) was added once more and then left on the orbital shaker for another 20 min. The resin was then washed six times with DMF.

Coupling Procedure for Amino Acids and Nala 24, 26. A solution of amino acid (3 equiv) and HATU (2.5 equiv) in DMF (2 mL) was prepared, then DIPEA (5 equiv) was added. The resulting yellow solution was added to the deprotected resin and left on the orbital shaker for 3 h. The resin was then filtered and washed in the following sequence: 3× DMF, 3× DCM, 3× *i*PrOH, 3× DCM, 3× *i*PrOH, 3× DCM.

Coupling Procedure for Nleu 28. A solution of bromoacetic acid (6.8 equiv) and DIC (8 equiv) in DMF (2 mL) was added to the deprotected resin and left on the orbital shaker for 1 h. The resin was then filtered and washed six times with DMF. A solution of isobutylamine (20 equiv) in DMF (2 mL) was then added to the resin and left on the orbital shaker for 1 h. The resin was then filtered and washed six times with DMF.

Cleavage and Deprotection Procedure. A 50% solution of trifluoroacetic acid (TFA) in DCM was added to the Wang resin (30% HFIP in DCM for 2-Cl chlorotrityl resin), and the mixture was left on the orbital shaker for 1 h. The solution was then filtered and concentrated under reduced pressure, adding DCM when dry (3×) to remove most of the TFA (or HFIP).

https://doi.org/10.1021/acs.jmedchem.0c02036
J. Med. Chem. 2021, 64, 5365−5383

Macrocyclization Procedure. The linear peptide was dissolved in DMF (0.025 mol/L), DEPBT was added (1.1 equiv), followed by DIPEA (3 equiv). The resulting yellow solution was left to stir until completion, typically around 72 h. It was then filtered on a carbonate scavenging cartridge and concentrated under reduced pressure. The crude product was purified on a preparative HPLC-MS.

Synthesis of Tether 7*S*. The 7*R* linker was synthesized using the same procedures.

5-Azidovaleric Acid 2. 5-Bromovaleric acid **1** (5.00 g, 27.6 mmol, 1 equiv) was dissolved in DMSO (275 mL, 0.1 M), sodium azide (7.18 g, 110 mmol, 4 equiv) was added, and the mixture was stirred overnight. Upon completion, 1 M HCl was added (300 mL) and the solution was extracted with ethyl acetate (3 × 300 mL). The organic phases were combined and washed with a 1:1 mixture of brine and 1 M HCl (6 × 300 mL), dried using $MgSO_4$, filtered, and concentrated under reduced pressure to obtain an orange oil (4.05 g, quantitative) that was used directly for the next step. ^{1}H NMR (300 MHz, $CDCl_3$): δ 11.42 (1H, s), 3.31 (2H, t, J = 6.6 Hz), 2.40 (2H, t, J = 7.2 Hz), 1.77−1.61 (4H, m); ^{13}C NMR (75 MHz, $CDCl_3$): δ 178.0, 51.0, 33.3, 28.2, 21.8; HRMS $[M - H]^-$ calcd for $C_5H_9N_3O_2$: 142.0611, found: 142.0621.

1-[(4*S*)-4-Benzyl-2-oxo-1,3-oxazolidin-3-yl]-5-azido-1-pentanone 3*S*. 5-Azidovaleric acid **2** (3.95 g, 27.6 mmol, 1 equiv) was dissolved in THF (92 mL, 0.3 M), and the solution was cooled to −78 °C. Triethylamine (4.62 mL, 33.1 mmol, 1.2 equiv) was added, followed by trimethylacetyl chloride (3.74 mL, 30.4 mmol, 1.1 equiv), and the solution was left to stir and warm up to 0 °C for 1 h. In a separate flask, (*S*)-4-benzyl-2-oxazolidinone (5.87 g, 33.1 mmol, 1.2 equiv) was dissolved in THF (39 mL, 0.7 M) and cooled to −78 °C. To this solution was added a solution of *n*-butyllithium in hexanes (33.1 mmol, 1.2 equiv) dropwise. The solution containing the azide was cooled back to −78 °C, and the oxazolidinone solution was added to it by a canula. It was left to stir and warm up to 0 °C for 2 h. When completed, the solution was poured into sat. NH_4Cl (300 mL) and extracted with EtOAc (3 × 300 mL). The organic fractions were merged, washed with brine (1 × 300 mL), dried using $MgSO_4$, filtered, and concentrated under reduced pressure to obtain an orange oil. This crude product was purified by flash chromatography (7:3 hexanes/ethyl acetate), yielding a colorless oil (6.06 g, 73%). ^{1}H NMR (300 MHz, $CDCl_3$): δ 7.40−7.25 (3H, m), 7.24−7.17 (2H, m), 4.74−4.63 (1H, m), 4.27−4.16 (3H, m), 3.39−3.25 (3H, m), 3.10−2.87 (2H, m); 1.87−1.64 (4H, m) ^{13}C NMR (75 MHz, $CDCl_3$): δ 172.3, 153.4, 135.2, 129.4, 128.9, 127.3, 66.2, 55.1, 51.1, 37.9, 34.9, 28.2, 21.3; HRMS $[M + Na]^+$ calcd for $C_{15}H_{18}N_4O_3$: 325.1271, found: 325.1278.

(2*S*)-1-[(4*S*)-4-Benzyl-2-oxo-1,3-oxazolidin-3-yl]-5-azido-2-methyl-1-pentanone 4*S*. 1-[(4*S*)-4-Benzyl-2-oxo-1,3-oxazolidin-3-yl]-5-azido-1-pentanone **3*S*** (6.06 g, 20.0 mmol, 1 equiv) was dissolved in THF (10 mL, 2 M) and cooled to −78 °C. In a separate vessel, a 0.5 M solution of potassium bis(trimethylsilyl)amide in toluene (56 mL, 28.1 mmol, 1.4 equiv) was dissolved in cold (−78 °C) THF (134 mL, 0.15 M). The solution containing the oxazolidinone was then added by a canula to the KHMDS solution and left to stir for 30 min. Methyl iodide (3.74 mL, 60 mmol, 3 equiv) was added, left to stir, and warmed up to 0 °C for 2 h. The reaction mixture was then poured into a saturated solution of NH_4Cl, and the product was extracted with ethyl acetate (3 × 500 mL). The organic fractions were merged, washed with brine (1 × 500 mL), dried using $MgSO_4$, filtered, and concentrated under reduced pressure to obtain a crude yellow oil (6.74 g, quant., de = 69%), which was used directly for the next step. ^{1}H NMR (300 MHz, $CDCl_3$): δ 7.40−7.25 (3H, m), 7.25−7.15 (2H, m), 4.75−4.65 (1H, m), 4.28−4.15 (2H, m), 3.82−3.67 (1H, m), 3.39−3.20 (3H, m), 2.78 (1H, dd, J = 13.1, 9.6 Hz), 1.92−1.77 (1H, m), 1.73−1.43 (3H, m), 1.26 (3H, d, J = 6.8 Hz) ^{13}C NMR (75 MHz, $CDCl_3$): δ 176.6, 153.0, 135.1, 129.4, 128.9, 127.4, 66.1, 55.2, 51.3, 37.9, 37.4, 30.3, 26.6, 17.5; HRMS $[M + Na]^+$ calcd for $C_{16}H_{20}N_4O_3$: 339.1428, found: 339.1430.

(2*S*)-5-Azido-2-methylvaleric Acid 5*S*. (2*S*)-1-[(4*S*)-4-Benzyl-2-oxo-1,3-oxazolidin-3-yl]-5-azido-2-methyl-1-pentanone **4*S*** (1.51 g, 4.77 mmol, 1 equiv) was dissolved in THF/H_2O (3:1, 100 mL, 0.05 M), and the solution was cooled to 0 °C. Hydrogen peroxide (2.70 mL, 23.8 mmol, 5 equiv) was added, followed by lithium hydroxide (228 mg, 9.52 mmol, 2 equiv) and the solution was left to stir until completion (approximately 20 min). A saturated solution of sodium sulfite was added (5 mL), and the solution was concentrated under reduced pressure to remove most of the THF. A saturated solution of sodium bicarbonate (100 mL) was added, and the product was washed with dichloromethane (3 × 100 mL). The aqueous phase was acidified to pH = 1 using 1 M HCl and extracted with ethyl acetate (3 × 100 mL). The ethyl acetate fractions were combined, dried using $MgSO_4$, filtered, and concentrated under reduced pressure to obtain a colorless oil (730 mg, 98%). ^{1}H NMR (300 MHz, $CDCl_3$): δ 10.61 (1H, s), 3.30 (2H, t, J = 6.6 Hz), 2.57−2.44 (1H, m), 1.83−1.48 (4H, m), 1.22 (3H, d, J = 6.9 Hz); ^{13}C NMR (75 MHz, $CDCl_3$): δ 182.2, 51.2, 38.9, 30.5, 26.5, 16.9; HRMS $[M - H]^-$ calcd for $C_6H_{11}N_3O_2$: 156.0768, found: 156.0772.

(2*S*)-5-Amino-2-methylvaleric Acid 6*S*. (2*S*)-5-Azido-2-methylvaleric acid **5*S*** (3.04 g, 19.3 mmol, 1 equiv) was dissolved in methanol (40 mL, 0.5 M) with 5% (v/v, 2 mL) acetic acid, palladium on carbon (10 wt %) was added (310 mg), and the solution was put under 300 psi of hydrogen and shaken for 16 h. The Pd/C was removed by filtration over a Celite pad, and the solution was concentrated under reduced pressure to obtain a colorless oil in quantitative yield. This crude product was used directly in the next step.

(2*S*)-2-Methyl-5-(*tert*-butoxycarbonylamino)valeric Acid 7*S*. (2*S*)-5-Amino-2-methylvaleric acid **6*S*** (2.54 g, 19.4 mmol, 1 equiv) was dissolved in a 2:1 mixture of dioxane and water (60 mL, 0.3 M) and sodium bicarbonate was added until pH reached 8. Di-*tert*-butyl dicarbonate (4.65 g, 21.3 mmol, 1.1 equiv) was added, and the solution was stirred for 16 h. Upon completion, the dioxane was removed under reduced pressure, 1 M HCl was added (100 mL), and the product was extracted with ethyl acetate (3 × 100 mL). The organic fractions were combined, dried using $MgSO_4$, filtered, and concentrated under reduced pressure to obtain a colorless oil (3.50 g, 78%). The product was isolated by flash chromatography (DCM/MeOH, 95:5) and coevaporated multiple times with toluene to yield a colorless oil (1.73 g, 39%). ^{1}H NMR (400 MHz, $CDCl_3$): δ 5.75 (0.2H, br s), 4.60 (0.8H, br s), 3.13 (2H, br t), 2.55−2.43 (1H, m), 1.77−1.63 (1H, m), 1.59−1.49 (3H, m), 1.45 (9H, s), 1.20 (3H, d, J = 7.0 Hz); ^{13}C NMR (100 MHz, $CDCl_3$): δ 181.8, 156.0, 79.3, 40.3, 39.0, 30.6, 28.4, 27.7, 16.9; HRMS $[M + Na]^+$ calcd for $C_{11}H_{21}NO_4$: 254.1363, found: 254.1368.

Synthesis of Tether 13*R*. The 13*S* linker was synthesized using the same procedures.

(3*R*)-3,7-Dimethyl-6-octenoic Acid 9*R*. (3*R*)-3,7-Dimethyl-6-octen-1-ol **8*R*** (5.00 g, 32.0 mmol, 1 equiv) was dissolved in DMF (100 mL, 0.3 M), and pyridinium dichromate (60.2 g, 160 mmol, 5 equiv) was added. The solution was stirred for 16 h. Upon completion, diethyl ether (300 mL) was added, and the mixture was washed with half-sat. NH_4Cl (6 × 300 mL) and brine (1 × 300 mL). The organic fractions were combined, dried using $MgSO_4$, filtered, and concentrated under reduced pressure to obtain a colorless oil. The product was isolated by flash chromatography (hexanes/EtOAc, 17:3) to yield a colorless oil (3.93 g, 72%). ^{1}H NMR (400 MHz, $CDCl_3$): δ 11.50 (1H, br s), 5.15−5.05 (1H, m), 2.38 (1H, dd, J = 15.4, 5.9 Hz), 2.16 (1H, dd, J = 15.4, 8.0 Hz), 2.07−1.92 (3H, m), 1.69 (3H, d, J = 1.0 Hz), 1.61 (3H, s), 1.45−1.34 (1H, m), 1.31−1.21 (1H, m), 0.99 (3H, d, J = 6.6 Hz); ^{13}C NMR (100 MHz, $CDCl_3$): δ 179.4, 131.7, 124.1, 41.5, 36.7, 29.8, 25.7, 25.4, 19.6, 17.6; HRMS $[M - H]^-$ calcd for $C_{10}H_{18}O_2$: 169.1223, found: 169.1233.

Methyl (3*R*)-3,7-Dimethyl-6-octenoate 10*R*. (3*R*)-3,7-Dimethyl-6-octenoic acid **9*R*** (2.51 g, 14.7 mmol, 1 equiv) was dissolved in diethyl ether (50 mL, 0.3 M). A solution of diazomethane (73.7 mmol, 5 equiv) in diethyl ether (200 mL, 0.37 M) was added, and the reaction was stirred for 2 h. Upon completion, drops of acetic acid were added until the solution became colorless. The solvent was concentrated by reduced pressure to yield a slightly yellow oil (2.60 g, 61%). ^{1}H NMR (300 MHz, $CDCl_3$): δ 5.14−5.04 (1H, m), 3.67 (3H, s), 2.33 (1H, dd, J = 14.8, 5.9 Hz), 2.12 (1H, dd, J = 15.2, 8.1 Hz), 2.06−1.87 (3H, m), 1.69 (3H, d, J = 0.9 Hz), 1.61 (3H, s), 1.43−1.16 (3H, m), 0.95 (3H, 6.6 Hz); ^{13}C NMR (75 MHz, $CDCl_3$): δ 173.7, 131.5, 124.2, 51.3, 41.6, 36.7, 30.0, 25.7, 25.4, 19.6, 17.6; HRMS $[M + Na]^+$ calcd for $C_{11}H_{20}O_2$: 207.1356, found: 207.1358.

(4*R*)-5-Methoxycarbonyl-4-methylvaleric Acid 11*R*. Methyl (3*R*)-3,7-dimethyl-6-octenoate **10*R*** (2.60 g, 14.1 mmol, 1 equiv) was

https://doi.org/10.1021/acs.jmedchem.0c02036
J. Med. Chem. 2021, 64, 5365−5383

dissolved in a 2:2:3 mixture of carbon tetrachloride (40 mL), acetonitrile (40 mL), and water (60 mL). Sodium periodate (12.4 g, 57.9 mmol, 4.1 equiv) was added, followed by ruthenium(III) chloride (65 mg, 0.31 mmol, 2.2 mol %). The resulting heterogeneous solution was stirred vigorously for 2 h or until completion. 1 M HCl was added, and the product was extracted with dichloromethane (3 × 200 mL). The organic fractions were combined and concentrated under reduced pressure, then resolubilized in ethyl acetate and extracted with dil. $NaHCO_3$ (3 × 200 mL). The aqueous phase was acidified to pH 1 using 1 M HCl and extracted with ethyl acetate (5 × 200 mL). The organic fractions from the last extraction were combined, dried using $MgSO_4$, filtered, and concentrated under reduced pressure to obtain a colorless oil (1.65 g, 67%). ^{1}H NMR (400 MHz, $CDCl_3$): δ 3.67 (3H, s), 2.46−2.26 (3H, m), 2.23−2.12 (1H, m), 2.07−1.93 (1H, m), 1.77−1.64 (1H, m), 1.61−1.47 (1H, m), 0.96 (3H, d, J = 6.7 Hz); ^{13}C NMR (100 MHz, $CDCl_3$): δ 179.0, 173.2, 51.5, 41.2, 31.5, 31.2, 29.8, 19.3; HRMS [M + Na]$^+$ calcd for $C_8H_{14}O_4$: 197.0784, found: 197.0786.

Methyl (3*R*)-3-Methyl-5-(*tert*-butoxycarbonylamino)-valerate 12*R*. (4*R*)-5-Methoxycarbonyl-4-methylvaleric acid **11*R*** (2.30 g, 13.2 mmol, 1 equiv) was dissolved in *tert*-butanol (130 mL, 0.1 M), then diphenylphosphoryl azide (3.13 mL, 14.5 mmol, 1.1 equiv) was added, followed by triethylamine (2.02 mL, 14.5 mmol, 1.1 equiv), and the mixture was refluxed for 16 h. Upon completion, the solvent was concentrated under reduced pressure and dissolved in ethyl acetate (100 mL). It was washed with half-sat. $NaHCO_3$ (2 × 100 mL), water (2 × 100 mL), and brine (1 × 100 mL). The organic fractions were combined, filtered through a pad of Celite, dried using $MgSO_4$, filtered, and concentrated under reduced pressure to obtain an orange oil (2.36 g, 73%), which was used without further purification. ^{1}H NMR (400 MHz, $CDCl_3$): δ 4.66 (1H, br s), 3.61 (3H, s), 3.18−2.95 (2H, m), 2.27 (1H, dd, J = 15.0, 6.3 Hz), 2.11 (1H, dd, J = 15.1, 7.7 Hz), 2.03−1.90 (1H, m), 1.52−1.41 (1H, m), 1.38 (9H, s), 1.35−1.28 (1H, m), 0.91 (3H, d, J = 6.7 Hz); HRMS [M + Na]$^+$ calcd for $C_{12}H_{23}NO_4$: 268.1519, found: 268.1518.

(3*R*)-3-Methyl-5-(*tert*-butoxycarbonylamino)valeric Acid 13*R*. Methyl (3*R*)-3-methyl-5-(*tert*-butoxycarbonylamino)valerate **12*R*** (571 mg, 2.33 mmol, 1 equiv) was dissolved in methanol (12 mL, 0.2 M), 1 M NaOH was added (12 mL, 12 mmol, 5 equiv), and the reaction was left to stir for 3 h. Upon completion, 1 M HCl was added to pH 2 and the product was extracted with dichloromethane (3 × 50 mL). The organic fractions were combined, dried using $MgSO_4$, filtered, and concentrated under reduced pressure to obtain a colorless oil (541 mg, quant.). The product was isolated by flash chromatography (DCM/MeOH, 19:1) to afford a colorless oil (484 mg, 90%). ^{1}H NMR (300 MHz, $CDCl_3$): δ 10.64 (1H, br s), 6.05 (0.3H, s), 4.67 (0.7H, s), 3.12 (2H, s), 2.43−2.26 (1H, m), 2.18 (1H, dd, J = 15.3, 7.5 Hz), 2.10−1.90 (1H, m), 1.65−1.48 (1H, m), 1.43 (9H, s), 0.98 (3H, 7.4 Hz); ^{13}C NMR (75 MHz, $CDCl_3$): 178.2, 156.1, 79.3, 41.3, 38.3, 36.5, 28.3, 27.5, 19.5; HRMS [M − H]$^-$ calcd for $C_{11}H_{21}NO_4$: 230.1387, found: 230.1388.

Synthesis of Tether 15*R*. The **15*S*** linker was synthesized using the same procedures.

(2*R*)-2,6-Dimethyl-5-heptenylamino 2,2-Dimethylpropionate 14*R*. (3*R*)-3,7-Dimethyl-6-octenoic acid **9*R*** (2.03 g, 11.9 mmol, 1 equiv) was dissolved in anhydrous THF (120 mL, 0.1 M), and the following reagents were added, in order: sodium azide (2.72 g, 3.5 equiv), zinc trifluoromethanesulfonate (143 mg, 0.394 mmol, 3.3 mol %), tetrabutylammonium bromide (577 mg, 1.79 mmol, 15 mol %), *tert*-butanol (571 μL, 5.97 mmol, 0.5 equiv), and di-*tert*-butyl dicarbonate (2.87 g, 13.13 mmol, 1.1 equiv) The mixture was left to stir for 16 h. Upon completion, a 10% w/v sodium nitrite solution was added (240 mL), followed by 120 mL of ethyl acetate and the mixture was left to stir for 10 min. The two phases were separated, and the remaining aqueous phase was extracted with further portions of ethyl acetate (3 × 120 mL). The organic phases were combined; washed with NH_4Cl (2 × 250 mL), $NaHCO_3$ (2 × 250 mL), and brine (1 × 250 mL); dried using $MgSO_4$; filtered; and concentrated under reduced pressure to obtain a yellow oil (2.76 g, 96%) The product was isolated by flash chromatography (hexanes/EtOAc, 9:1) to afford a colorless oil (1.30 g, 45%). ^{1}H NMR (400 MHz, $CDCl_3$): δ 5.13−5.04 (1H, m), 4.55 (1H, s), 3.15−2.80 (2H, m), 2.09−1.90 (2H, m), 1.68 (3H, d, J = 0.9 Hz); 1.66−1.54 (1H, m), 1.60 (3H, s), 1.45 (9H, s), 1.42−1.31 (1H, m), 1.20−1.07 (1H, m), 0.90 (3H, d, J = 6.8 Hz); ^{13}C NMR (75 MHz, $CDCl_3$): 156.1, 131.5, 124.4, 79.0, 46.5, 34.3, 33.2, 28.4, 25.7, 25.3, 17.6, 17.4; HRMS [M + Na]$^+$ calcd for $C_{14}H_{27}NO_2$: 264.1934, found: 264.1939.

(4*R*)-4-Methyl-5-(*tert*-butoxycarbonylamino)valeric Acid 15*R*. (2*R*)-2,6-Dimethyl-5-heptenylamino 2,2-dimethylpropionate **14*R*** (2.40 g, 9.96 mmol, 1 equiv) was dissolved in methanol (50 mL, 0.2 M) and chilled to −78 °C. Ozone was bubbled through the solution for 45 min followed by oxygen for 30 min. The flask was removed from the cooling bath, and 30% hydrogen peroxide was added (5.64 mL, 49.7 mmol, 5 equiv), followed by 1 M sodium hydroxide (20 mL, 19.9 mmol, 2 equiv), and it was left to stir for 16 h. Upon completion, the flask was chilled to 0 °C and a saturated solution of sodium sulfite (5 mL) was added dropwise to quench excess peroxides. The solution was acidified to pH 2 using 1 M HCl and extracted with dichloromethane (3 × 50 mL). The organic phases were combined, dried using $MgSO_4$, filtered, and concentrated under reduced pressure to obtain a slightly yellow oil (2.33 g, quant.), and the product was isolated by flash chromatography (hexanes/EtOAc/formic acid, 98:1:1−95:4:1) and then coevaporated five times with toluene to remove traces of formic acid to afford a slightly yellow oil (1.29 g, 56%). ^{1}H NMR (400 MHz, $CDCl_3$): δ 12.50−8.10 (1H, br s), 5.95 (0.3H, s), 4.67 (0.7H, s), 3.15−2.92 (2H, m), 2.51−2.27 (2H, m), 1.82−1.58 (2H, m), 1.45 (9H, s), 0.92 (3H, d, J = 6.7 Hz); ^{13}C NMR (75 MHz, $CDCl_3$): 178.8, 156.2, 79.3, 46.0, 33.2, 31.5, 28.8, 28.4, 17.1; HRMS [M + Na]$^+$ calcd for $C_{11}H_{21}NO_4$: 254.1363, found: 254.1368.

Synthesis of Tether 22*R*. The **22*S*** linker was synthesized using the same procedures.

(1*S*)-3-Diazo-1-methyl-2-oxopropylamino 2,2-Dimethylpropionate 17*R*. Boc-L-Ala-OH **16*R*** (1.00 g, 5.29 mmol, 1 equiv) was dissolved in anhydrous THF (21 mL, 0.25 M), and the solution was cooled to −15 °C. Isobutylchloroformate (564 μL, 5.81 mmol, 1.1 equiv) was added, followed by triethylamine (420 μL, 5.81 mmol, 1.1 equiv) After 15 min of stirring, it was removed from the cooling bath and left to warm up to room temperature. The resulting white mixture was filtered on a pad of Celite to obtain a colorless solution. To this solution was slowly added a freshly prepared solution of diazomethane in ether (30 mL, 0.88 M, 5 equiv), and the resulting yellow solution was left to stir for 2.5 h. Upon completion, the solution was quenched with acetic acid until colorless. It was then washed twice with sat. $NaHCO_3$ (2 × 60 mL), sat. NH_4Cl (2 × 60 mL), and brine (1 × 60 mL). The organic phase was dried using $MgSO_4$, filtered, and concentrated under reduced pressure to obtain a yellow oil (>100%). This crude product was purified by flash chromatography (4:1 hexanes/ethyl acetate) to obtain a yellow crystalline solid (718 mg, 64%). ^{1}H NMR (300 MHz, $CDCl_3$): δ 5.44 (1H, s), 5.12 (1H, s), 4.23 (1H, s), 1.45 (9H, s), 1.33 (3H, d, J = 7.0 Hz); ^{13}C NMR (75 MHz, $CDCl_3$): δ 194.4, 155.1, 80.0, 53.4, 28.3, 18.5; HRMS [M + Na]$^+$ calcd for $C_9H_{15}N_3O_3$: 236.1006, found: 236.1010.

Methyl (3*S*)-3-(*tert*-Butoxycarbonylamino)butyrate 18*R*. (1*S*)-3-Diazo-1-methyl-2-oxopropylamino 2,2-dimethylpropionate **17*R*** (718 mg, 3.37 mmol, 1.0 equiv) was dissolved in anhydrous methanol (34 mL, 0.1 M). To this was added dropwise a solution of silver benzoate (78 mg, 0.34 mmol, 0.1 equiv) in triethylamine (3.4 mL, 0.1 M with respect to silver benzoate). After about 5 min, the solution turned black and was left to stir overnight. Upon completion, the solution was filtered on Celite and concentrated under reduced pressure to yield an orange oil, which was solubilized in ethyl acetate (30 mL); washed with water (1 × 30 mL), 0.1 M HCl (1 × 30 mL), and brine (1 × 30 mL); dried using $MgSO_4$; filtered; and concentrated under reduced pressure to obtain a black oil. This crude product was purified by flash chromatography (3:1 hexanes/ethyl acetate) to obtain a yellow solid (628 mg, 86%). ^{1}H NMR (300 MHz, $CDCl_3$): δ 4.91 (1H, s), 4.03 (1H, m), 3.68 (3H, s), 2.50 (2H, m), 1.43 (9H, s), 1.21 (3H, d, J = 6.6 Hz); ^{13}C NMR (75 MHz, $CDCl_3$): δ 172.0, 155.0, 79.3, 51.6, 43.4, 40.6, 28.4, 20.4; HRMS [M + Na]$^+$ calcd for $C_{10}H_{19}NO_4$: 240.1206, found: 240.1212.

https://doi.org/10.1021/acs.jmedchem.0c02036
J. Med. Chem. 2021, 64, 5365−5383

(1*S*)-2-Formyl-1-methylethylamino 2,2-Dimethylpropionate 19*R*. Methyl (3*S*)-3-(*tert*-butoxycarbonylamino)butyrate **18*R*** (1.53 g, 7.05 mmol, 1 equiv) was dissolved in anhydrous dichloromethane (14 mL, 0.5 M) and chilled to −78 °C. To this was added a 1 M diisobutylaluminium hydride solution (12.0 mL, 12.0 mmol, 1.7 equiv) dropwise. Upon completion, the reaction mixture was transferred into a saturated solution of potassium sodium tartrate (50 mL) and the mixture was left to stir for 1 h. The two phases were separated, and the aqueous phase was extracted with dichloromethane (3 × 50 mL). The organic phases were combined, dried using $MgSO_4$, filtered, and concentrated under reduced pressure to obtain a yellow oil. The product was isolated by flash chromatography (DCM/MeOH, 99:1) to afford a slightly yellow oil (1.05 g, 86%). ^{1}H NMR (300 MHz, $CDCl_3$): δ 9.76 (1H, t, J = 1.9 Hz), 4.69 (1H, s), 4.23−3.98 (1H, m), 2.70−2.47 (2H, m), 1.43 (9H, s), 1.24 (3H, d, J = 6.6 Hz); ^{13}C NMR (75 MHz, $CDCl_3$): δ 155.1, 79.6, 50.6, 42.3, 28.3, 21.0, aldehyde signal not observed; HRMS $[M + Na]^+$ calcd for $C_{11}H_{21}NO_4$: 210.1101, found: 210.1104.

Ethyl (5*S*,*E*)-5-(*tert*-Butoxycarbonylamino)-2-hexenoate 20*R*. Triethyl 2-phosphonoacetate **19*R*** (1.41 mL, 7.05 mmol, 1.1 equiv) was dissolved in anhydrous THF (8 mL, 0.8 M), sodium hydride (200 mg, 8.33 mmol, 1.3 equiv) was added, and the mixture was left to stir for 1 h. In a separate vessel, (1*S*)-2-formyl-1-methylethylamino 2,2-dimethylpropionate (1.11 g, 6.41 mmol, 1 equiv) was dissolved in anhydrous THF (3.2 mL, 2 M). This solution was then added dropwise to the first solution and left to stir for 1 h. Upon completion, water (10 mL) was added and the product was extracted with dichloromethane (5 × 20 mL). The organic phases were combined, dried using $MgSO_4$, filtered, and concentrated under reduced pressure to obtain a slightly yellow oil. This crude product was purified by flash chromatography (hexanes/ethyl acetate, 17:3) to afford a colorless oil (1.11 g, 68%). ^{1}H NMR (300 MHz, $CDCl_3$): δ 6.90 (1H, dt, J = 15.6, 7.5 Hz), 5.86 (1H, dt, J = 15.6, 1.3 Hz), 4.41 (1H, s), 4.18 (2H, q, J = 7.1 Hz), 3.81 (1H, s), 2.40−2.30 (2H, m), 1.43 (9H, s), 1.28 (3H, t, J = 7.1 Hz), 1.14 (3H, d, J = 6.6 Hz); ^{13}C NMR (75 MHz, $CDCl_3$): δ 166.2, 155.1, 144.6, 124.0, 79.3, 60.3, 45.6, 39.5, 28.3, 20.6, 14.2; HRMS $[M + Na]^+$ calcd for $C_{13}H_{23}NO_4$: 280.1519, found: 280.1525.

(5*S*,*E*)-5-(*tert*-Butoxycarbonylamino)-2-hexenoic Acid 21*R*. Ethyl (5*S*,*E*)-5-(*tert*-butoxycarbonylamino)-2-hexenoate **20*R*** (989 mg, 3.84 mmol, 1 equiv) was dissolved in a 1:1 mixture of water and methanol (40 mL, 0.1 M), sodium hydroxide (768 mg, 19.2 mmol, 5 equiv) was added, and the solution was stirred for 2 h. Upon completion, the methanol was largely removed under reduced pressure and 1 M HCl (20 mL) was added to pH 2. The product was extracted with dichloromethane (3 × 40 mL). The organic phases were combined, dried using $MgSO_4$, filtered, and concentrated under reduced pressure to obtain a white solid (807 mg, 92%) that was used without further purification. ^{1}H NMR (300 MHz, $CDCl_3$): δ 9.77 (1H, br s), 7.01 (1H, dt, J = 15.6, 7.5 Hz), 5.87 (1H, dt, J = 15.6, 1.3 Hz), 4.48 (1H, s), 3.84 (1H, s), 2.45−2.30 (2H, m), 1.44 (9H, s), 1.16 (3H, d, J = 6.6 Hz); HRMS $[M + Na]^+$ calcd for $C_{11}H_{19}NO_4$: 252.1206, found: 252.1212.

(5*S*)-5-(*tert*-Butoxycarbonylamino)hexanoic Acid 22*R*. (5*S*,*E*)-5-(*tert*-Butoxycarbonylamino)-2-hexenoic acid **21*R*** (807 mg, 3.52 mmol, 1 equiv) was dissolved in methanol (35 mL, 0.1 M), palladium on carbon (10 wt %) was added (15 mg), and the solution was put under hydrogen atmosphere and shaken for 16 h. Upon completion, the reaction mixture was filtered through a pad of Celite and concentrated under reduced pressure to afford a colorless oil (796 mg, 98%). ^{1}H NMR (300 MHz, $CDCl_3$): δ 5.56 (0.3H, s), 4.39 (0.7H, s), 3.66 (1H, s), 2.37 (2H, td, J = 7.4, 2.0 Hz), 1.81−1.57 (3H, m), 1.50−1.41 (3H, m), 1.45 (9H, s), 1.13 (3H, d, J = 6.6 Hz); ^{13}C NMR (75 MHz, $CDCl_3$): δ 178.5, 155.4, 79.2, 53.4, 46.1, 36.5, 33.6, 28.4, 21.2; HRMS $[M + Na]^+$ calcd for $C_{11}H_{21}NO_4$: 254.1363, found: 254.1369.

(3*S*,6*S*,9*S*)-3-Benzyl-6-isobutyl-9-methyl-1,4,7,10-tetraza-2,5,8,11-cyclopentadecanetetrone (Ø-Ø). ^{1}H NMR (400 MHz, MeOD): δ 7.32−7.16 (5H, m), 4.46 (1H, dd, J = 11.5, 4.2 Hz), 4.04−3.89 (2H, m), 3.53−3.38 (2H, m), 3.07 (1H, dd, J = 14.4, 11.3 Hz), 3.02−2.93 (1H, m), 2.30−2.20 (1H, m), 2.12−2.03 (1H, m), 1.79−1.66 (3H, m), 1.66−1.58 (3H, m), 1.58−1.49 (3H, m), 1.47 (3H, d, J = 7.2 Hz), 1.40−1.30 (1H, m), 0.87 (3H, d, J = 6.3 Hz), 0.82 (3H, d, J = 6.5 Hz); ^{13}C NMR (100 MHz, MeOD): δ 176.6, 176.5, 174.5, 173.5, 139.6, 130.3, 129.6, 127.7, 56.8, 55.5, 52.3, 40.8, 39.7, 37.7, 36.1, 28.1, 26.1, 23.3, 22.9, 22.1, 16.5; HRMS $[M + Na]^+$ calcd for $C_{23}H_{34}N_4O_4$: 453.2472, found: 453.2473.

(6*S*,9*S*)-4-Benzyl-6-isobutyl-9-methyl-1,4,7,10-tetraza-2,5,8,11-cyclopentadecanetetrone (Nphe-Ø). ^{1}H NMR (400 MHz, MeOD): δ 7.33−7.15 (5H, m), 4.79−4.72 (1H, q, J = 7 Hz), 4.50−4.42 (1H, m), 4.28 (1H, d, J = 14.2 Hz), 3.59−3.52 (1H, m), 3.28−3.12 (3H, m), 2.94−2.85 (1H, dd, J = 13.6, 10.1 Hz), 2.29−2.19 (1H, m), 2.11−2.03 (1H, m), 1.99−1.87 (1H, m), 1.83−1.70 (1H, m), 1.67−1.54 (2H, m), 1.53−1.41 (2H, m), 1.32 (3H, d, J = 7 Hz), 0.98 (3H, d, J = 6.7 Hz), 0.92 (3H, d, J = 6.8 Hz), 0.85−0.77 (1H, m); ^{13}C NMR (400 MHz, MeOD): δ 174.8, 172.6, 170.8, 169.1, 138.6, 129.1, 128.9, 128.2, 126.3, 126.2, 56.1, 55.2, 51.3, 44.3, 37.6, 36.2, 34.1, 27.4, 27.1, 25.5, 23.0, 20.0, 19.9, 19.8, 19.7, 17.2; HRMS $[M + Na]^+$ calcd for $C_{23}H_{34}N_4O_4$: 453.2472, found: 453.2465.

(3*S*,9*S*)-3-Benzyl-7-isobutyl-9-methyl-1,4,7,10-tetraza-2,5,8,11-cyclopentadecanetetrone (Nleu-Ø). ^{1}H NMR (300 MHz, MeOD): δ 7.36−7.19 (5H, m), 4.74−4.66 (1H, m), 4.44−4.35 (1H, m), 4.07−3.97 (1H, m), 3.66−3.57 (1H, d, J = 15.0 Hz), 3.56−3.39 (2H, m), 3.16−3.01 (1H, m), 3.01−2.88 (2H, m), 2.83−2.70 (1H, m), 2.25−2.12 (1H, m), 2.05−1.35 (5H, m), 1.35−1.15 (3H, m), 0.89 (3H, d, J = 6.6 Hz), 0.83 (3H, d, J = 6.6 Hz); ^{13}C NMR (75 MHz, MeOD): δ 177.2, 174.7, 174.2, 173.7, 139.2, 130.4, 130.2, 129.7, 129.6, 127.8, 56.0, 55.0, 54.7, 40.9, 40.0, 39.6, 38.9, 35.7, 32.1, 27.9, 25.9, 23.4, 22.9, 22.7, 22.5, 21.6; HRMS $[M + Na]^+$ calcd for $C_{23}H_{34}N_4O_4$: 453.2472, found: 453.2470.

(3*S*,6*S*)-3-Benzyl-6-isobutyl-10-methyl-1,4,7,10-tetraza-2,5,8,11-cyclopentadecanetetrone (Nala-Ø). ^{1}H NMR (400 MHz, DMSO-d_6): δ 8.15 (1H, d, J = 6.3 Hz), 7.97 (1H, d, J = 8.5 Hz), 7.43−7.35 (2H, m), 7.33−7.26 (1H, m), 7.22−7.15 (2H, m), 6.97 (1H, t, J = 5.3 Hz), 5.00 (1H, d, J = 17.1 Hz), 4.54−4.45 (1H, m), 4.45−4.34 (2H, m), 4.10−4.01 (1H, m), 3.23 (1H, d, J = 15.7 Hz), 3.20−2.98 (2H, m), 2.28−2.19 (1H, m), 2.03−1.88 (1H, m), 1.69−1.54 (1H, m), 1.54−1.42 (4H, m), 1.42−1.30 (2H, m), 1.22 (3H, d, J = 7.3 Hz), 0.69 (3H, d, J = 6.3 Hz), 0.67 (3H, d, J = 6.2 Hz); ^{13}C NMR (100 MHz,): δ 172.1, 167.5, 137.4, 128.8, 127.4, 126.6, 51.6, 51.0, 50.4, 47.0, 40.7, 40.4, 37.6, 34.2, 27.4, 23.9, 22.9, 22.4, 21.9, 17.0; HRMS $[M + Na]^+$ calcd for $C_{23}H_{34}N_4O_4$: 453.2472, found: 453.2468.

(3*S*,6*S*,9*S*,12*R*)-3-Benzyl-6-isobutyl-9,12-dimethyl-1,4,7,10-tetraza-2,5,8,11-cyclopentadecanetetrone (Ø-2R). ^{1}H NMR (400 MHz, DMSO-d_6): δ 8.70 (1H, d, J = 7.5 Hz), 8.24 (1H, s), 8.02 (1H, s), 7.32−7.13 (5H, m), 6.72 (1H, d, J = 6.7 Hz), 6.59 (1H, d, J = 7.9 Hz), 4.41−4.31 (1H, m), 4.96−4.84 (2H, m), 2.95−2.72 (2H, m), 2.23−2.11 (1H, m), 1.69−1.56 (1H, m), 1.54−1.43 (2H, m), 1.40 (3H, d, J = 7.0 Hz), 1.37−1.10 (5H, m), 1.00 (3H, d, J = 6.8 Hz), 0.81 (3H, d, J = 6.5 Hz); ^{13}C NMR (100 MHz, DMSO-d_6): δ 176.0, 173.8, 171.6, 170.7, 138.5, 128.9, 128.1, 126.1, 53.9, 49.9, 40.8, 37.7, 36.7, 30.1, 25.9, 24.2, 22.6, 21.4, 18.3, 16.8; HRMS $[M + Na]^+$ calcd for $C_{23}H_{34}N_4O_4$: 467.2629, found: 467.2638.

(3*S*,6*S*,9*S*,12*S*)-3-Benzyl-6-isobutyl-9,12-dimethyl-1,4,7,10-tetraza-2,5,8,11-cyclopentadecanetetrone (Ø-2S). ^{1}H NMR (400 MHz, DMSO-d_6): δ 8.13 (1H, d, J = 8.0 Hz, H_N Phe), 7.91 (1H, d, J = 7.9 Hz, H_N Ala), 7.81 (1H, d, J = 8.4 Hz, H_N Leu), 7.50−7.43 (1H, m, H_N Linker), 7.30−7.13 (5H, m), 4.23−4.10 (2H, m, H_α Phe and H_α Ala), 4.03 (1H, td, J = 8.4, 6.3 Hz, H_α Leu), 3.27−3.18 (1H, m, H_5 Linker), 3.17−3.07 (1H, m, H_β Phe), 2.90 (1H, dd, J = 13.8, 9.1 Hz, H_β Phe), 2.39−2.29 (1H, m, H_2 Linker), 1.49−1.38 (3H, m, H_β Leu and H_4 Linker), 1.37−1.28 (4H, m, H_β Leu, H_γ Leu and H_3 Linker), 1.23 (3H, d, J = 7.3 Hz, H_β Ala), 0.95 (3H, d, J = 6.8 Hz, H_{Me} Linker), 0.81 (3H, d, J = 6.3 Hz, H_δ Leu), 0.78 (3H, d, J = 6.2 Hz, H_δ Leu); ^{1}H NMR (400 MHz, $CDCl_3$): δ 7.59 (1H, br s, H_N Phe), 7.34−7.16 (5H, m), 6.57 (1H, s, H_N Leu), 6.39 (2H, s, H_N Ala and H_N Linker), 4.79−4.57 (1H, m, H_α Phe), 4.22−4.08 (1H, m, H_α Ala), 3.90 (1H, br s, H_α Leu), 3.67−3.52 (1H, m, H_5 Linker), 3.46 (1H, dd, J = 14.0, 5.0 Hz, H_β Phe), 3.04−2.94 (1H, m, H_β Phe), 2.93−2.86 (1H, br s, H_5 Linker), 2.48−2.36 (1H, m, H_2 Linker), 1.57−1.51 (3H, m, H_β Leu and H_3 Linker), 1.49 (3H, d, J = 7.0 Hz, H_β Ala), 1.45−1.35 (1H, m, H_γ Leu),

https://doi.org/10.1021/acs.jmedchem.0c02036
J. Med. Chem. 2021, 64, 5365−5383

1.32−1.21 (1H, m), 1.13 (3H, d, J = 4.6 Hz, H_{Me} Linker), 0.86 (3H, d, J = 6.5 Hz, H_δ Leu), 0.80 (3H, d, J = 6.5 Hz, H_δ Leu); ^{13}C NMR (100 MHz, DMSO-d_6): δ 175.3, 172.7, 171.1, 170.3, 138.3, 129.0, 128.1, 126.2, 55.1, 52.9, 49.5, 41.1, 38.1, 37.7, 36.2, 30.6, 25.0, 24.2, 22.4, 22.2, 17.7, 15.3; HRMS [M + Na]$^+$ calcd for $C_{23}H_{34}N_4O_4$: 467.2629, found: 467.2640.

(6*S*,9*S*,12*R*)-4-Benzyl-6-isobutyl-9,12-dimethyl-1,4,7,10-tetraza-2,5,8,11-cyclopentadecanetetrone (Nphe-2R). ^{1}H NMR (400 MHz, DMSO-d_6): δ 8.37 (1H, d, J = 8.0 Hz), 8.27 (1H, d, J = 5.3 Hz), 7.43−7.34 (2H, m), 7.34−7.26 (1H, m), 7.22−7.13 (2H, m), 7.03−6.95 (1H, m), 5.07 (1H, d, J = 17.1 Hz), 4.46−4.28 (2H, m), 4.28−4.19 (1H, m), 4.05−3.94 (1H, m), 3.16 (1H, d, J = 16.2 Hz), 3.04−2.82 (2H, m), 2.20−2.10 (1H, m), 2.06−1.95 (1H, m), 1.82−1.68 (1H, m), 1.68−1.54 (1H, m), 1.54−1.37 (3H, m), 1.22 (3H, d, J = 7.2 Hz), 0.87 (3H, d, J = 6.7 Hz), 0.73 (3H, d, J = 2.7 Hz), 0.72 (3H, d, J = 2.6 Hz); ^{13}C NMR (100 MHz, DMSO-d_6): δ 174.2, 173.1, 171.5, 167.6, 137.4, 128.8, 127.4, 126.7, 51.3, 50.7, 50.4, 47.8, 44.1, 40.2, 31.7, 31.4, 29.5, 24.0, 22.9, 21.9, 18.1, 16.6; HRMS [M + Na]$^+$ calcd for $C_{23}H_{34}N_4O_4$: 467.2629, found: 467.2624.

(6*S*,9*S*,12*S*)-4-Benzyl-6-isobutyl-9,12-dimethyl-1,4,7,10-tetraza-2,5,8,11-cyclopentadecanetetrone (Nphe-2S). ^{1}H NMR (400 MHz, DMSO-d_6): δ 8.77 (1H, d, J = 6.2 Hz, H_N Leu), 8.06 (1H, d, J = 8.7 Hz, H_N Ala), 7.46−7.12 (5H, m), 6.89 (1H, s, H_N Linker), 5.32 (1H, br s), 5.18 (1H, d, J = 15 Hz), 4.68−4.57 (1H, m, H_α Phe), 4.56−4.47 (1H, m, H_α Ala), 4.40−4.21 (1H, m, H_α Leu), 3.77 (1H, d, J = 15.0 Hz, H_β Phe), 3.21−3.09 (1H, m, H_5 Linker), 3.00−2.90 (1H, m, H_5 Linker), 2.69−2.68 (m, 1H), 2.48−2.38 (1H, m, H_2 Linker), 2.35−2.30 (1H, dt, 3.7, 1.8 Hz), 1.70−1.58 (1H, m, H_4 Linker), 1.58−1.48 (1H, m, H_β Leu), 1.48−1.39 (1H, m, H_γ Leu), 1.33−1.21 (3H, m, H_3 Linker), 1.17 (3H, d, J = 7.0 Hz, H_β Ala), 1.14−1.07 (1H, m, H_4 Linker), 0.93 (3H, d, J = 6.7 Hz, H_{Me} Linker), 0.91−0.83 (2H, m), 0.66 (3H, d, J = 6.3 Hz, H_δ Leu), 0.41 (3H, d, J = 4.3 Hz, H_δ Leu); ^{1}H NMR (400 MHz, $CDCl_3$): δ 7.41−7.17 (5H, m), 6.98 (1H, br s, H_N Leu), 6.57−6.47 (1H, m, H_N Linker), 5.87 (1H, d, J = 7.7 Hz, H_N Ala), 5.34 (1H, d, J = 17.1 Hz, H_β Phe), 4.81−4.73 (1H, m, H_α Leu), 4.70 (1H, d, J = 14.9 Hz, H_α Nphe), 4.57−4.54 (1H, m, H_α Ala), 4.50 (1H, d, J = 17.1 Hz, H_β Nphe), 3.51−3.41 (1H, m, H_5 Linker), 3.34 (1H, d, J = 14.9 Hz, H_α Nphe), 3.08−2.95 (1H, m, H_5 Linker), 2.27−2.12 (1H, m, H_2 Linker), 1.64−1.57 (2H, m, H_3 Linker), 1.54−1.40 (3H, m, H_4 Linker and H_γ Leu), 1.36 (3H, d, J = 6.8 Hz, H_β Ala), 1.15 (3H, d, J = 6.7 Hz, H_{Me} Linker), 0.76 (3H, d, J = 6.7 Hz, H_δ Leu), 0.59 (3H, d, J = 6.5 Hz, H_δ Leu); ^{13}C NMR (100 MHz, DMSO-d_6): δ 174.9, 168.0, 138.0, 128.8, 128.5, 127.6, 127.3, 126.5, 52.5, 38.6, 37.5, 31.6, 25.8, 23.7, 23.1, 22.9, 22.0, 20.9, 19.7, 18.1, 17.2, 15.1; HRMS [M + Na]$^+$ calcd for $C_{23}H_{34}N_4O_4$: 467.2629, found: 467.2622.

(3*S*,9*S*,12*R*)-3-Benzyl-7-isobutyl-9,12-dimethyl-1,4,7,10-tetraza-2,5,8,11-cyclopentadecanetetrone (Nleu-2R). ^{1}H NMR (400 MHz, DMSO-d_6): δ 8.79 (1H, d, J = 9.2 Hz), 8.41 (1H, s), 8.31 (1H, d, J = 8.5 Hz), 8.21 (1H, d, J = 1.9 Hz), 7.78−7.68 (1H, d, J = 7.9 Hz), 7.48−7.39 (1H, m), 7.32−7.14 (10H, m), 4.69−4.55 (2H, m), 4.48−4.38 (1H, m), 4.32−4.23 (2H, m), 4.20−4.09 (1H, d, J = 18.3 Hz), 3.20−3.11 (2H, m), 3.10−3.01 (2H, m), 3.00−2.81 (2H, m), 2.80−2.69 (2H, m), 2.27−2.03 (3H, m), 1.95−1.82 (1H, m), 1.79−1.52 (4H, m), 1.47−1.28 (3H, m), 1.21 (3H, d, J = 7.0 Hz), 1.17 (3H, d, J = 6.7 Hz), 1.08 (3H, d, J = 7.2 Hz), 0.93 (3H, d, J = 6.8 Hz), 0.89 (3H, d, J = 6.7 Hz), 0.82 (3H, d, J = 6.7 Hz), 0.75 (3H, d, J = 6.7 Hz), 0.68 (3H, d, J = 6.7 Hz); ^{13}C NMR (100 MHz, DMSO-d_6): δ 176.2, 175.6, 174.02, 170.4, 169.1, 167.9, 138.7, 138.3, 129.2, 129.0, 128.2, 128.1, 126.2, 55.5, 55.0, 54.9, 53.8, 50.7, 44.6, 42.0, 38.4, 36.2, 31.6, 30.8, 27.2, 26.5, 25.8, 20.1, 19.9, 19.7, 17.2, 16.7, 16.4; HRMS [M + Na]$^+$ calcd for $C_{23}H_{34}N_4O_4$: 467.2629, found: 467.2625.

(3*S*,9*S*,12*S*)-3-Benzyl-7-isobutyl-9,12-dimethyl-1,4,7,10-tetraza-2,5,8,11-cyclopentadecanetetrone (Nleu-2S). ^{1}H NMR (400 MHz, DMSO-d_6): δ 8.36 (1H, d, J = 8.2 Hz, H_N Phe), 7.99 (1H, d, J = 8.0 Hz, H_N Ala), 7.46−7.36 (1H, m, H_N Linker), 7.30−7.15 (5H, m), 4.72−4.65 (1H, m, H_α Ala), 4.25−4.19 (1H, m, H_α Phe), 4.16 (1H, d, J = 14.0 Hz, H_α Nleu), 3.48−3.39 (1H, m, H_β Nleu), 3.29−3.24 (1H, m, H_α Nleu), 3.19−3.11 (1H, m, H_β Phe), 3.11−3.08 (1H, m, H_β Nleu), 3.07−2.96 (2H, m, H_5 Linker), 2.75 (1H, dd, J = 14.3, 10.9 Hz, H_β Phe), 2.34−2.31 (1H, m, H_2 Linker), 1.93−1.85 (1H, m, H_γ Nleu), 1.71−1.61 (2H, m, H_4 Linker), 1.25−1.22 (2H, m, H_3 Linker), 1.20 (3H, d, J = 6.8 Hz, H_β Ala), 0.91 (3H, d, J = 6.7 Hz, H_{Me} Linker), 0.90 (3H, d, J = 6.3 Hz, H_δ Nleu), 0.84 (3H, d, J = 6.7 Hz, H_α Nleu); ^{1}H NMR (400 MHz, $CDCl_3$): δ 7.34−7.19 (5H, m), 7.25 (1H, d, J = 7.2 Hz, H_N Phe), 6.39 (1H, d, J = 8.9 Hz, H_N Ala), 5.70 (1H, br s, H_N Linker), 5.05−4.95 (1H, m, H_α Ala), 4.67 (1H, dd, J = 13.5, 0.9 Hz, H_α Nleu), 4.50 (1H, dt, J = 9.2, 7.5 Hz, H_α Phe), 3.61−3.49 (1H, m, H_5 Linker), 3.44 (1H, dd, J = 14.4, 8.0 Hz, H_β Nleu), 3.15 (1H, d, J = 13.7 Hz, H_α Nleu), 3.09−3.05 (2H, m, H_β Phe), 3.03−2.94 (1H, m, H_β Nleu), 2.84−2.75 (1H, m, H_5 Linker), 2.47−2.38 (1H, m, H_2 Linker), 1.96−1.85 (1H, m, H_γ Nleu), 1.59−1.51 (2H, m, H_4 Linker), 1.35 (3H, d, J = 6.7 Hz, H_β Ala), 1.33−1.25 (3H, m, H_3 Linker), 1.08 (3H, d, J = 6.7 Hz, H_{Me} Linker), 0.95 (3H, d, J = 6.7 Hz, H_δ Nleu), 0.92 (3H, d, J = 6.8 Hz, H_δ Nleu); ^{13}C NMR (100 MHz, DMSO-d_6): δ 175.4, 175.0, 171.0, 169.4, 138.7, 129.1, 128.9, 128.3, 128.2, 126.3, 56.3, 55.5, 51.4, 44.2, 37.8, 36.2, 32.0, 27.5, 26.0, 20.0, 19.9, 19.8, 17.4, 17.2; HRMS [M + Na]$^+$ calcd for $C_{23}H_{34}N_4O_4$: 467.2629, found: 467.2626.

(3*S*,6*S*,12*R*)-3-Benzyl-6-isobutyl-10-methyl-12-methyl-1,4,7,10-tetraza-2,5,8,11-cyclopentadecanetetrone (Nala-2R). ^{1}H NMR (400 MHz, DMSO-d_6): δ 8.84 (1H, d, J = 5.5 Hz), 7.37 (1H, d, J = 9.4 Hz), 7.32−7.13 (5H, m), 6.36 (1H, d, J = 9.4 Hz), 4.46−4.35 (1H, m), 4.28 (1H, d, J = 15.0 Hz), 3.83−3.73 (1H, m), 3.60 (1H, d, J = 15.0 Hz), 3.21 (3H, s), 2.95−2.86 (1H, m), 2.86−2.79 (1H, m), 2.71−2.62 (1H, m), 1.82−1.68 (1H, m), 1.65−1.53 (1H, m), 1.48−1.36 (1H, m), 1.32−1.05 (4H, m), 0.97 (3H, d, J = 6.7 Hz), 0.80 (3H, d, J = 6.5 Hz), 0.74 (3H, 6.5 Hz); ^{13}C NMR (100 MHz, DMSO-d_6): δ 178.1, 172.8, 171.9, 171.1, 138.8, 129.2, 128.7, 126.7, 54.1, 53.5, 40.6, 40.4, 40.2, 39.7, 39.5, 39.3, 39.2, 25.0, 24.5, 23.3, 21.3, 18.8; HRMS [M + Na]$^+$ calcd for $C_{23}H_{34}N_4O_4$: 467.2629, found: 467.2626.

(3*S*,6*S*,12*S*)-3-Benzyl-6-isobutyl-10-methyl-12-methyl-1,4,7,10-tetraza-2,5,8,11-cyclopentadecanetetrone (Nala-2S). ^{1}H NMR (400 MHz, DMSO-d_6): δ 8.29 (1H, d, J = 4.3 Hz, H_N Leu), 8.06 (1H, d, J = 8.7 Hz, H_N Phe), 7.32−7.11 (5H, m), 6.87 (1H, dd, J = 6.7, 2.2 Hz, H_N Linker), 4.49 (1H, d, J = 17.8 Hz, H_α Nala), 4.34 (1H, ddd, J = 11.2, 8.8, 4.1 Hz, H_α Phe), 3.81 (1H, d, J = 17.7 Hz, H_α Nala), 3.82−3.75 (1H, m, H_α Leu), 3.29−3.23 (2H, m, H_β Phe and H_5 Linker), 2.84 (1H, dd, J = 14.1, 11.4 Hz), 2.83−2.78 (1H, m, H_5 Linker), 2.72 (3H, s, H_{Me} Linker), 2.69−2.65 (1H, m, H_2 Linker), 1.62−1.50 (1H, m, H_3 Linker), 1.47−1.38 (2H, m, H_4 Linker), 1.36−1.22 (2H, m, H_β Leu and H_γ Leu), 1.21−1.06 (2H, m, H_β Leu and H_3 Linker), 0.96 (3H, d, J = 6.7 Hz, H_{Me} Linker), 0.79 (3H, d, J = 6.2 Hz, H_δ Leu), 0.71 (3H, d, J = 6.3 Hz, H_δ Leu); ^{1}H NMR (400 MHz, $CDCl_3$): δ 7.42 (1H, br s, H_N Phe), 7.35−7.13 (1H, br s, N_H Linker and N_H Leu), 4.65 (1H, br s, H_α Phe), 4.13−3.98 (1H, m), 3.86 (1H, br s, H_α Leu), 3.62−3.48 (2H, m, H_5 Linker), 3.47−3.38 (1H, m, H_β Phe), 3.18 (3H, s, H_β Nala), 3.13−3.04 (2H, m, H_5 Linker and H_β Phe), 2.93 (2H, s), 2.89−2.78 (1H, m, H_2 Linker), 1.80−1.66 (2H, br s, H_3 Linker), 1.54−1.45 (1H, br s, H_γ Leu), 1.16 (3H, d, J = 6.7 Hz, H_{Me} Linker), 0.95−0.78 (6H, m, H_δ Leu); ^{13}C NMR (100 MHz, DMSO-d_6): δ 175.9, 171.8, 170.8, 169.9, 138.6, 128.9, 128.0, 126.0, 54.0, 53.9, 51.2, 35.9, 34.8, 34.4, 30.3, 23.8, 22.2, 17.1; HRMS [M + Na]$^+$ calcd for $C_{23}H_{34}N_4O_4$: 467.2629, found: 467.2632.

(3*S*,6*S*,9*S*,13*R*)-3-Benzyl-6-isobutyl-9,13-dimethyl-1,4,7,10-tetraza-2,5,8,11-cyclopentadecanetetrone (Ø-3R). ^{1}H NMR (400 MHz, DMSO-d_6): δ 8.22−8.06 (3H, m), 7.54 (1H, t, J = 5.3 Hz), 7.29−7.11 (5H,m), 4.20−4.12 (1H, m), 3.95−3.86 (1H, m), 3.28−3.18 (1H, m), 3.13 (1H, dd, J = 13.8, 5.2 Hz), 2.99−2.88 (2H, m), 2.14−2.04 (1H, m), 1.92−1.83 (1H, m), 1.74−1.61 (1H, m), 1.53−1.23 (5H, m), 1.21 (3H, d, J = 7.3 Hz), 0.89 (3H, d, J = 6.8 Hz), 0.82−0.73 (6H, m); ^{13}C NMR (100 MHz, DMSO-d_6): δ 172.9, 172.3, 171.2, 170.4, 138.5, 129.0, 128.1, 126.1, 55.3, 53.1, 49.9, 42.4, 40.4, 40.0, 36.4, 36.0, 35.6, 28.5, 24.3, 22.5, 22.2, 20.9, 17.2; HRMS [M + Na]$^+$ calcd for $C_{23}H_{34}N_4O_4$: 467.2629, found: 467.2639.

(3*S*,6*S*,9*S*,13*S*)-3-Benzyl-6-isobutyl-9,13-dimethyl-1,4,7,10-tetraza-2,5,8,11-cyclopentadecanetetrone (Ø-3S). ^{1}H NMR (400 MHz, DMSO-d_6): δ 8.52 (1H, d, J = 7 Hz), 8.17−8.05 (1H, m), 8.05−7.93 (1H, m), 7.30−7.13 (5H, m), 6.90−6.80 (1H, m), 4.39−4.30 (1H, m), 4.08−3.91 (2H, m), 3.27 (1H, dd, J = 13.9, 4.5 Hz), 2.87−2.75 (2H, m), 2.21 (1H, d, J = 10.8 Hz), 1.89−1.63 (3H, m), 1.49−1.38 (1H, m), 1.38−1.34 (1H, m), 1.32 (3H, d, J = 7.2 Hz),

https://doi.org/10.1021/acs.jmedchem.0c02036
J. Med. Chem. 2021, 64, 5365−5383

1.26−1.15 (1H, m), 1.15−1.03 (1H, m), 0.93 (3H, d, J = 6.2 Hz), 0.80 (3H, d, J = 6.5 Hz), 0.73 (3H, d, J = 6.3 Hz); ^{13}C NMR (100 MHz, DMSO-d_6): δ 173.2, 172.1, 171.5, 170.2, 138.4, 128.9, 128.1, 126.1, 53.9, 53.2, 50.0, 43.4, 36.5, 35.8, 34.8, 27.4, 24.2, 22.5, 21.7, 21.0, 17.2; HRMS [M + Na]$^+$ calcd for $C_{23}H_{34}N_4O_4$: 467.2629, found: 467.2644.

(6*S*,9*S*,13*R*)-4-Benzyl-6-isobutyl-9,13-dimethyl-1,4,7,10-tetraza-2,5,8,11-cyclopentadecanetetrone (Nphe-3R). ^{1}H NMR (400 MHz, DMSO-d_6): δ 8.24 (1H, d, J = 6.2 Hz), 7.65 (1H, d, J = 9.2 Hz) 7.42−7.34 (2H, m), 7.33−7.26 (1H, m), 7.23−7.12 (2H, m), 7.01−6.91 (1H, m), 6.55 (3H, br s), 4.99 (1H, d, J = 17.3 Hz), 4.80−4.70 (1H, m), 4.46 (1H, d, J = 17.1 Hz), 4.34 (1H, d, J = 16.1 Hz), 4.06−3.96 (1H, m), 3.30−3.19 (1H, m), 3.13−3.02 (1H, m), 2.23 (1H, d, J = 12.5 Hz), 1.85−1.75 (2H, m), 1.74−1.62 (1H, m), 1.51−1.40 (1H, m), 1.40−1.15 (2H, m), 1.23 (3H, d, J = 7.2 Hz), 0.93 (3H, d, J = 6.5 Hz), 0.65 (3H, d, J = 6.5 Hz), 0.60 (3H, d, J = 6.5 Hz); ^{13}C NMR (100 MHz, DMSO-d_6): δ 172.8, 172.6, 172.5, 167.3, 137.5, 128.8, 127.4, 126.4, 51.7, 51.5, 50.6, 45.9, 42.3, 40.9, 40.4, 36.1, 34.7, 28.0, 23.9, 23.9, 22.9, 21.8, 21.6, 17.1; HRMS [M + Na]$^+$ calcd for $C_{23}H_{34}N_4O_4$: 467.2629, found: 467.2622.

(6*S*,9*S*,13*S*)-4-Benzyl-6-isobutyl-9,13-dimethyl-1,4,7,10-tetraza-2,5,8,11-cyclopentadecanetetrone (Nphe-3S). ^{1}H NMR (400 MHz, DMSO-d_6): δ 8.69 (1H, s), 8.10 (1H, s), 7.46−7.06 (5H, m), 6.87 (1H, s), 6.66 (1H, s), 5.34 (1H, s), 4.68−4.44 (1H, m), 4.44−4.14 (2H, m), 2.93 (2H, s), 2.14−1.64 (3H, m), 1.63−1.35 (3H, m), 1.21−1.00 (3H, m), 0.90 (3H, d, J = 6.8 Hz), 0.65 (2H, s), 0.36 (2H, s); ^{13}C NMR (100 MHz, DMSO-d_6): δ 175.1, 173.5, 172.0, 168.0, 138.0, 128.7, 127.3, 126.4, 51.9, 47.5, 42.1, 38.6, 35.8, 33.6, 29.6, 29.3, 24.2, 23.7, 23.0, 22.1, 20.8, 18.4, 17.5; HRMS [M + Na]$^+$ calcd for $C_{23}H_{34}N_4O_4$: 467.2629, found: 467.2621.

(3*S*,9*S*,13*R*)-3-Benzyl-7-isobutyl-9,13-dimethyl-1,4,7,10-tetraza-2,5,8,11-cyclopentadecanetetrone (Nleu-3R). ^{1}H NMR (400 MHz, DMSO-d_6): δ 8.23 (1H, d, J = 8.5 Hz), 8.05 (1H, d, J = 7.3 Hz), 7.51−7.41 (1H, m), 7.30−7.12 (6H, m), 4.64−4.52 (1H, m), 4.32−4.22 (1H, m), 4.18 (1H, d, J = 14.0 Hz), 3.22 (1H, d, J = 14.0 Hz), 3.20−3.11 (2H, m), 3.10−2.97 (2H, m), 2.76 (1H, dd, J = 14.5, 10.7 Hz), 2.10 (1H, dd, J = 12.2, 9.6 Hz), 1.93−1.73 (3H, m), 1.63−1.50 (1H, m), 1.19 (3H, d, J = 6.8 Hz), 1.14−1.02 (1H, m), 0.92−0.85 (6H, m), 0.82 (3H, d, J = 6.7 Hz); ^{13}C NMR (100 MHz, DMSO-d_6): δ 174.8, 172.0, 171.0, 169.0, 138.6, 128.9, 128.24, 128.19, 126.2, 56.1, 55.1, 51.3, 44.6, 42.3, 36.3, 35.9, 34.1, 29.0, 27.3, 20.6, 19.8, 19.7, 17.1; HRMS [M + Na]$^+$ calcd for $C_{23}H_{34}N_4O_4$: 467.2629, found: 467.2626.

(3*S*,9*S*,13*S*)-3-Benzyl-7-isobutyl-9,13-dimethyl-1,4,7,10-tetraza-2,5,8,11-cyclopentadecanetetrone (Nleu-3S). ^{1}H NMR (400 MHz, DMSO-d_6): δ 8.36−8.25 (1H, m), 8.21−8.14 (1H, m), 8.08−7.96 (1H, m), 7.66−7.57 (1H, m), 7.36−7.29 (1H, m), 7.29−7.12 (6H, m), 4.75−4.57 (1H, m), 4.46−4.30 (1H, m), 4.27−4.16 (1H, m), 3.65−3.53 (1H, m), 3.28−3.17 (3H, m), 3.17−3.05 (2H, m), 3.03−2.86 (2H, m), 2.82−2.69 (1H, m), 2.39−2.27 (1H, m), 2.16−2.02 (1H, m), 2.00−1.55 (5H, m), 1.31−1.15 (2H, m), 1.16 (3H, dd, J = 18.9, 6.8 Hz), 0.97−0.87 (6H, m), 0.71 (3H, dd, J = 26.0, 6.7 Hz); ^{13}C NMR (100 MHz, DMSO-d_6): δ 175.1, 172.9, 172.4, 172.1, 170.7, 170.5, 169.9, 168.5, 139.2, 129.5, 129.4, 128.6, 128.5, 126.7, 126.6, 56.4, 55.8, 55.3, 53.4, 51.8, 51.6, 44.8, 44.6, 43.0, 42.2, 40.6, 40.4, 40.2, 39.9, 39.7, 39.5, 39.3, 37.7, 37.1, 36.7, 35.7, 35.1, 30.0, 29.1, 27.7, 26.2, 22.1, 21.7, 20.6, 20.30, 20.25, 20.2, 18.1, 17.9; HRMS [M + Na]$^+$ calcd for $C_{23}H_{34}N_4O_4$: 467.2629, found: 467.2630.

(3*S*,6*S*,13*R*)-3-Benzyl-6-isobutyl-10-methyl-13-methyl-1,4,7,10-tetraza-2,5,8,11-cyclopentadecanetetrone (Nala-3R). ^{1}H NMR (400 MHz, DMSO-d_6): δ 8.44 (1H, s), 8.32−8.15 (1H, m), 7.61 (1H, s), 7.31−7.06 (5H, m), 4.51−4.35 (2H, m), 3.97−3.86 (1H, m), 3.81 (1H, d, J = 18.1 Hz), 3.22−3.11 (1H, m), 3.11−2.93 (2H, m), 2.75 (3H, s), 2.39 (1H, d, J = 12.5 Hz), 1.92−1.71 (2H, m), 1.63−1.44 (1H, m), 1.41−1.19 (3H, m), 1.19−1.06 (1H, m), 0.80 (3H, d, J = 6.3 Hz), 0.77 (3H, d, J = 6.0 Hz), 0.71 (3H, 6.3 Hz); HRMS [M + Na]$^+$ calcd for $C_{23}H_{34}N_4O_4$: 467.2629, found: 467.2626.

(3*S*,6*S*,13*S*)-3-Benzyl-6-isobutyl-10-methyl-13-methyl-1,4,7,10-tetraza-2,5,8,11-cyclopentadecanetetrone (Nala-3S). ^{1}H NMR (400 MHz, DMSO-d_6): δ 8.85 (1H, d, J = 5.5 Hz), 8.51−8.35 (1H, m), 7.31−7.11 (9H, m), 6.50−6.40 (1H, m), 4.50−4.18 (3H, m), 4.00−3.89 (1H, m), 3.82−3.73 (1H, m), 3.60 (1H, d, J = 15.0 Hz), 3.19 (3H, s), 2.75−2.66 (3H, m), 1.97−1.90 (1H, m), 1.84−1.66 (2H, m), 1.63−1.51 (1H, m), 1.45−1.33 (1H, m), 1.31−1.25 (1H, m), 1.22−1.16 (3H, m), 1.16−1.04 (1H, m), 0.98 (3H, d, J = 6.8 Hz), 0.83−0.70 (13H, m), 0.67 (2H, d, J = 6.3 Hz); ^{13}C NMR (100 MHz, DMSO-d_6): δ 174.1, 172.2, 171.4, 170.5, 138.2, 133.7, 129.0, 128.7, 128.2, 128.0, 126.2, 53.5, 53.1, 53.0, 40.4, 38.5, 37.2, 36.7, 34.8, 34.1, 28.2, 24.0, 23.7, 22.8, 22.4, 22.1, 21.2, 20.9, 19.1; HRMS [M + Na]$^+$ calcd for $C_{23}H_{34}N_4O_4$: 467.2629, found: 467.2631.

(3*S*,6*S*,9*S*,14*R*)-3-Benzyl-6-isobutyl-9,14-dimethyl-1,4,7,10-tetraza-2,5,8,11-cyclopentadecanetetrone (Ø-4R). ^{1}H NMR (400 MHz, DMSO-d_6): δ 8.28−8.12 (3H, m), 7.70−7.60 (1H, m), 7.29−7.13 (5H, m), 4.36−4.24 (1H, m), 4.08−3.96 (2H, m), 3.21−3.08 (2H, m), 2.88 (1H, dd, J = 14.0, 9.1 Hz), 2.70−2.59 (1H, m), 2.13−2.00 (2H, m), 1.77−1.62 (1H, m), 1.51−1.36 (2H, m), 1.34−1.13 (3H, m), 1.21 (3H, d, J = 7.2 Hz), 0.86−0.77 (6H, m), 0.75 (3H, 6.2 Hz); ^{13}C NMR (100 MHz, DMSO-d_6): δ 173.7, 172.9, 171.2, 170.1, 138.2, 129.0, 128.1, 126.2, 55.0, 54.9, 53.1, 50.3, 44.6, 40.8, 36.6, 33.2, 32.8, 29.8, 24.3, 22.5, 22.0, 18.0, 17.2; HRMS [M + Na]$^+$ calcd for $C_{23}H_{34}N_4O_4$: 467.2629, found: 467.2641.

(3*S*,6*S*,9*S*,14*S*)-3-Benzyl-6-isobutyl-9,14-dimethyl-1,4,7,10-tetraza-2,5,8,11-cyclopentadecanetetrone (Ø-4S). ^{1}H NMR (400 MHz, DMSO-d_6): δ 8.48 (1H, d, J = 6.7 Hz), 8.18 (1H, s), 8.05 (1H, s), 7.30−7.12 (7H, m), 4.41−4.30 (1H, m), 4.07−3.90 (2H, m), 3.27−3.17 (1H, m), 3.14−3.01 (1H, m), 2.86−2.68 (2H, m), 2.26−2.16 (1H, m), 1.75−1.63 (1H, m), 1.48−1.37 (1H, m), 1.31 (3H, d, J = 7.2 Hz), 1.27−1.17 (1H, m), 1.13−1.01 (1H, m), 0.85 (3H, d, J = 6.7 Hz), 0.79 (3H, d, J = 6.3 Hz), 0.73 (3H, d, J = 6.3 Hz); ^{13}C NMR (100 MHz, DMSO-d_6): δ 173.1, 173.0, 171.4, 170.3, 138.3, 128.9, 128.1, 126.1, 54.2, 53.3, 50.0, 44.1, 40.2, 36.8, 32.2, 31.8, 29.6, 24.2, 22.5, 21.8, 17.6, 17.1; HRMS [M + Na]$^+$ calcd for $C_{23}H_{34}N_4O_4$: 467.2629, found: 467.2613.

(6*S*,9*S*,14*R*)-4-Benzyl-6-isobutyl-9,14-dimethyl-1,4,7,10-tetraza-2,5,8,11-cyclopentadecanetetrone (Nphe-4R). ^{1}H NMR (400 MHz, DMSO-d_6): δ 7.98 (1H, d, J = 8.5 Hz), 7.63 (1H, d, J = 8.0 Hz), 7.45−7.12 (7H, m), 6.86−6.75 (1H, m), 4.97 (1H, d, J = 17.1 Hz), 4.68−4.57 (1H, m), 4.55−4.36 (2H, m), 4.26−4.17 (1H, m), 3.18−3.07 (1H, m), 3.01−2.79 (2H, m), 2.22−2.10 (1H, m), 1.64−1.36 (6H, m), 1.33−1.10 (9H, m), 1.03−0.92 (1H, m), 0.90−0.75 (2H, m), 0.68 (3H, d, J = 6.5 Hz), 0.63 (3H, d, J = 6.3 Hz); ^{13}C NMR (100 MHz, DMSO-d_6): δ 175.0, 172.8, 172.5, 167.6, 137.3, 128.8, 127.5, 126.5, 51.8, 51.4, 49.9, 41.3, 40.8, 37.9, 32.1, 26.6, 23.9, 23.0, 21.7, 17.5, 16.8; HRMS [M + Na]$^+$ calcd for $C_{23}H_{34}N_4O_4$: 467.2629, found: 467.2623.

(6*S*,9*S*,14*S*)-4-Benzyl-6-isobutyl-9,14-dimethyl-1,4,7,10-tetraza-2,5,8,11-cyclopentadecanetetrone (Nphe-4S). ^{1}H NMR (400 MHz, DMSO-d_6): δ 8.20 (1H, d, J = 6.2 Hz), 7.86 (1H, d, J = 8.7 Hz), 7.48−7.34 (2H, m), 7.34−7.24 (1H, m), 7.24−7.13 (2H, m), 7.12−7.01 (1H, m), 4.93 (1H, d, J = 17.1 Hz), 4.74−4.57 (1H, m), 4.51−4.32 (2H, m), 4.10−3.97 (1H, m), 3.27 (1H, d, J = 15.7 Hz), 3.12−2.98 (1H, m), 2.95−2.79 (1H, m), 2.37−2.21 (1H, m), 2.06−1.78 (2H, m), 1.65−1.26 (5H, m), 1.22 (3H, d, J = 7.3 Hz), 0.83 (3H, d, J = 6.7 Hz), 0.75−0.55 (6H, m); ^{13}C NMR (100 MHz, DMSO-d_6): δ 173.3, 172.8, 172.5, 167.5, 137.4, 128.8, 127.4, 126.5, 51.5, 51.0, 50.4, 46.4, 43.7, 40.7, 31.4, 30.9, 29.2, 24.0, 22.8, 22.0, 17.8, 17.1; HRMS [M + Na]$^+$ calcd for $C_{23}H_{34}N_4O_4$: 467.2629, found: 467.2621.

(3*S*,9*S*,14*R*)-3-Benzyl-7-isobutyl-9,14-dimethyl-1,4,7,10-tetraza-2,5,8,11-cyclopentadecanetetrone (Nleu-4R). ^{1}H NMR (400 MHz, DMSO-d_6): δ 8.12−7.99 (2H, m), 7.44−7.34 (1H, m), 7.31−7.10 (6H, m), 4.53−4.43 (1H, m), 4.34−4.24 (1H, m), 4.18 (1H, d, J = 14.2 Hz), 3.24−3.12 (2H, m), 3.11−2.99 (1H, m), 2.99−2.76 (3H, m), 2.19−1.94 (2H, m), 1.93−1.72 (4H, m), 1.49−1.30 (2H, m), 1.19 (3H, d, J = 6.7 Hz), 1.12 (1H, d, J = 6.3 Hz), 1.09−1.00 (1H, m), 0.94−0.83 (7H, m), 0.81 (3H, d, J = 6.5 Hz), 0.77−0.64 (2H, m); ^{13}C NMR (100 MHz, DMSO-d_6): δ 174.8, 173.3, 170.6, 168.5, 138.6, 129.1, 128.9, 128.1, 126.1, 56.0, 54.9, 54.7, 51.5, 45.2, 45.0, 36.3, 33.0, 31.2, 30.7, 27.4, 19.9, 19.79, 19.75, 18.7, 16.6; HRMS [M + Na]$^+$ calcd for $C_{23}H_{34}N_4O_4$: 467.2629, found: 467.2620.

(3*S*,9*S*,14*S*)-3-Benzyl-7-isobutyl-9,14-dimethyl-1,4,7,10-tetraza-2,5,8,11-cyclopentadecanetetrone (Nleu-4S). ^{1}H NMR (400 MHz, DMSO-d_6): δ 8.39 (1H, dd, J = 70.7, 6.42 Hz), 8.00

https://doi.org/10.1021/acs.jmedchem.0c02036
J. Med. Chem. 2021, 64, 5365−5383

(1H, dd, J = 46.4, 8.4 Hz), 7.87 (1H, dt, J = 84.4, 5.5 Hz), 7.31−7.11 (5H, m), 4.68 (1H, dt, J = 51.1, 7.2 Hz), 4.25 (1H, dd, J = 120.0, 18 Hz), 4.35 (1H, m), 3.19−2.72 (6H, m), 2.07 (1H, dm, 181.8 Hz), 2.06−1.21 (6H, m), 1.14 (3H, dd, J = 28.1, 6.6 Hz), 0.90−0.75 (6H, m), 0.68 (3H, dd, J = 11.0, 6.7 Hz); HRMS [M + Na]+ calcd for $C_{23}H_{34}N_4O_4$: 467.2629, found: 467.2622.

(3*S*,6*S*,14*R*)-3-Benzyl-6-isobutyl-10-methyl-14-methyl-1,4,7,10-tetraza-2,5,8,11-cyclopentadecanetetrone (Nala-4R). ^{1}H NMR (400 MHz, DMSO-d_6): δ 8.07 (1H, d, J = 6.5 Hz), 7.90 (1H, d, J = 8.9 Hz), 7.53−7.45 (1H, m), 7.27−7.10 (5H, m), 4.47−4.30 (2H, m), 3.97−3.89 (1H, m), 3.86 (1H, d, J = 18.1 Hz), 3.28−3.18 (1H, m), 3.15 (1H, s), 3.11−3.03 (1H, m), 2.75 (3H, s), 2.35−2.22 (1H, m), 2.13−2.03 (1H, m), 1.67−1.55 (1H, m), 1.55−1.43 (1H, m), 1.43−1.35 (1H, m), 1.35−1.25 (1H, m), 1.20−1.07 (2H, m), 0.88−0.78 (6H, m), 0.77−0.69 (3H, d, J = 6.5 Hz); ^{13}C NMR (100 MHz, DMSO-d_6): δ 173.4, 171.8, 170.7, 168.9, 138.0, 129.1, 128.8, 128.2, 128.0, 126.1, 54.1, 53.4, 52.1, 45.2, 40.1, 37.2, 34.7, 32.6, 32.1, 30.7, 24.1, 22.4, 21.9, 18.7; HRMS [M + Na]$^+$ calcd for $C_{23}H_{34}N_4O_4$: 467.2629, found: 467.2628.

(3*S*,6*S*,14*S*)-3-Benzyl-6-isobutyl-10-methyl-14-methyl-1,4,7,10-tetraza-2,5,8,11-cyclopentadecanetetrone (Nala-4S). ^{1}H NMR (400 MHz, DMSO-d_6): δ 8.58 (1H, d, J = 5.5 Hz), 8.21 (1H, m), 7.98 (1H, d, J = 8.5 Hz), 7.14−6.88 (11H, m), 6.33 (1H, d, J = 9.1 Hz), 4.25−3.99 (3H, m), 3.71−3.61 (1H, m), 3.60−3.51 (1H, m), 3.37 (1H, d, J = 15.0 Hz), 3.23−3.14 (2H, m), 3.04−2.92 (2H, m), 2.97 (3H, s), 2.87−2.73 (1H, m), 2.56 (2H, d, J = 13.3 Hz), 2.33 (1H, d, J = 11.8 Hz), 2.27 (2H, s), 2.21−2.07 (1H, m), 1.98−1.86 (1H, m), 1.80−1.70 (1H, m), 1.53−1.21 (3H, m), 1.21−0.81 (6H, m), 0.73 (2H, d, J = 6.7 Hz), 0.66 (2H, d, J = 6.7 Hz), 0.56 (5H, 6.3 Hz), 0.53−0.43 (5H, m); ^{13}C NMR (100 MHz, DMSO-d_6): δ 174.9, 172.8, 172.1, 171.8, 171.4, 170.35, 170.31, 169.6, 138.4, 138.2, 129.05, 128.98, 128.7, 128.2, 128.00, 127.96, 126.2, 126.1, 53.9, 52.9, 52.1, 45.6, 44.5, 39.8, 39.04, 39.02, 37.2, 36.1, 34.4, 32.9, 30.7, 29.8, 29.5, 29.1, 24.0, 23.9, 22.8, 22.2, 20.9, 18.5, 17.9; HRMS [M + Na]$^+$ calcd for $C_{23}H_{34}N_4O_4$: 467.2629, found: 467.2627.

(3*S*,6*S*,9*S*,15*R*)-3-Benzyl-6-isobutyl-9,15-dimethyl-1,4,7,10-tetraza-2,5,8,11-cyclopentadecanetetrone (Ø-5R). ^{1}H NMR (400 MHz, MeOD): δ 7.33−7.14 (5H, m), 4.56 (1H, dd, J = 11.4, 3.9 Hz), 4.10−4.02 (1H, m), 3.89−3.76 (2H, m), 3.47 (1H, dd, J = 14.7, 3.9 Hz), 2.98 (1H, dd, J = 15.4, 11.7 Hz), 2.22 (1H, dt, J = 13.3, 3.9 Hz), 2.05 (1H, td, J = 13.0, 3.4 Hz), 1.75−1.61 (2H, m), 1.53 (3H, d, J = 7.2 Hz), 1.52−1.38 (3H, m), 1.38−1.27 (2H, m), 1.10 (3H, d, J = 6.5 Hz), 0.87 (3H, d, J = 6.5 Hz), 0.81 (3H, d, J = 6.5 Hz); ^{13}C NMR (100 MHz, MeOD): δ 176.5, 176.4, 174.7, 172.9, 139.6, 130.2, 129.6, 127.7, 56.1, 55.7, 52.4, 46.8, 40.8, 38.2, 36.2, 35.5, 26.1, 23.3, 22.9, 22.0, 21.9, 16.3; HRMS [M + Na]$^+$ calcd for $C_{23}H_{34}N_4O_4$: 467.2629, found: 467.2640.

(3*S*,6*S*,9*S*,15*S*)-3-Benzyl-6-isobutyl-9,15-dimethyl-1,4,7,10-tetraza-2,5,8,11-cyclopentadecanetetrone (Ø-5S). ^{1}H NMR (400 MHz, MeOD): δ 7.31−7.16 (5H, m), 4.14−4.02 (2H, m), 3.79−3.68 (1H, m), 3.58−3.52 (1H, m), 3.49−3.33 (2H, m), 2.20−2.04 (2H, m), 1.84−1.56 (5H, m), 1.55−1.40 (2H, m), 1.33 (3H, d, J = 7.3 Hz), 1.16 (3H, d, J = 6.7 Hz), 0.91 (3H, d, J = 6.7 Hz), 0.87 (3H, d, J = 6.5 Hz); ^{13}C NMR (100 MHz, MeOD): δ 175.6, 175.4, 172.3, 171.3, 138.8, 128.7, 128.0, 126.1, 90.0 58.0, 53.4, 50.3, 45.9, 37.5, 34.5, 34.2, 33.4, 24.7, 22.1, 21.6, 20.4, 20.0, 15.1; HRMS [M + Na]$^+$ calcd for $C_{23}H_{34}N_4O_4$: 467.2629, found: 467.2630.

(6*S*,9*S*,15*R*)-4-Benzyl-6-isobutyl-9,15-dimethyl-1,4,7,10-tetraza-2,5,8,11-cyclopentadecanetetrone (Nphe-5R). ^{1}H NMR (400 MHz, MeOD): δ 7.49−7.24 (5H, m), 4.99−4.90 (2H, m), 4.67 (1H, d, J = 16.7 Hz), 4.41 (1H, d, J = 16.6 Hz), 4.24 (1H, q, J = 7.3 Hz), 3.79−3.69 (1H, m), 3.60 (1H, d, J = 16.4 Hz), 2.45−2.36 (1H, m), 2.04−1.94 (1H, m), 1.85−1.73 (1H, m), 1.64−1.44 (5H, m), 1.38 (3H, d, J = 7.3 Hz), 1.31−1.21 (1H, m), 0.99 (3H, d, J = 6.5 Hz), 0.78 (3H, d, J = 6.5 Hz), 0.72 (3H, d, 6.5 Hz); ^{13}C NMR (100 MHz, MeOD): δ 177.2, 176.0, 175.6, 138.1, 130.5, 129.3, 128.4, 54.4, 53.7, 52.3, 49.3, 47.3, 42.7, 36.0, 35.2, 26.0, 24.4, 23.7, 22.3, 22.1, 17.1; HRMS [M + Na]$^+$ calcd for $C_{23}H_{34}N_4O_4$: 467.2629, found: 467.2625.

(6*S*,9*S*,15*S*)-4-Benzyl-6-isobutyl-9,15-dimethyl-1,4,7,10-tetraza-2,5,8,11-cyclopentadecanetetrone (Nphe-5S). ^{1}H NMR (400 MHz, MeOD): δ 7.45−7.35 (2H, m), 7.35−7.28 (1H, m), 7.28−7.18 (2H, m), 5.27 (1H, d, J = 17.4 Hz), 4.69 (1H, dd, J = 16.5, 1.2 Hz), 4.42 (1H, d, J = 17.4 Hz), 4.21 (1H, q, J = 7.2 Hz), 4.00 (1H, dd, J = 8.6, 5.7 Hz), 3.78−3.67 (1H, m), 3.25 (1H, d, J = 16.6 Hz), 2.21−2.11 (2H, m), 1.81−1.49 (7H, m), 1.35 (3H, d, J = 7.2 Hz), 1.14 (3H, d, J = 6.5 Hz), 0.88−0.79 (6H, m); ^{13}C NMR (100 MHz, MeOD): δ 177.4, 176.1, 173.8, 170.7, 138.1, 130.3, 129.0, 127.8, 53.3, 52.3, 52.0, 51.5, 47.5, 41.8, 36.1, 34.9, 25.8, 24.4, 23.6, 22.3, 21.7, 16.9; HRMS [M + Na]$^+$ calcd for $C_{23}H_{34}N_4O_4$: 467.2629, found: 467.2630.

(3*S*,9*S*,15*R*)-3-Benzyl-7-isobutyl-9,15-dimethyl-1,4,7,10-tetraza-2,5,8,11-cyclopentadecanetetrone (Nleu-5R). ^{1}H NMR (400 MHz, DMSO-d_6): δ 8.06−7.94 (1H, m), 7.83−7.68 (1H, m), 7.68−7.50 (2H, m), 7.30−7.11 (5H, m), 6.96 (1H, s), 4.79−4.62 (1H, m), 4.61−4.51 (1H, m), 4.49−4.35 (1H, m), 3.84−3.67 (1H, m), 3.60−3.44 (1H, m), 3.21−3.03 (2H, m), 3.01−2.88 (1H, m),2.87−2.74 (1H, m), 2.34−2.17 (1H, m), 2.14−1.92 (1H, m), 1.90−1.71 (2H, m), 1.58−1.30 (3H, m), 1.31−1.20 (1H, m), 1.16 (2H, d, J = 6.4 Hz), 1.06 (2H, d, J = 6.6 Hz), 0.91 (2H, d, J = 6.6 Hz), 0.88−0.83 (2H, m), 0.83−0.78 (2H, d, J = 6.6 Hz), 0.74−0.64 (3H, m); ^{13}C NMR (100 MHz, DMSO-d_6): δ 173.2, 172.1, 172.0, 171.3, 170.2, 169.6, 168.5, 168.1, 138.3, 137.7, 129.1, 128.14, 128.10, 126.3, 126.2, 55.5, 54.5, 54.2, 54.1, 52.9, 50.1, 43.4, 43.1, 42.8, 40.4, 37.4, 35.7, 35.3, 34.6, 34.0, 33.2, 27.1, 25.5, 22.6, 21.6, 21.4, 20.1, 20.04, 19.96, 19.8, 19.4, 17.9, 17.5; HRMS [M + Na]$^+$ calcd for $C_{23}H_{34}N_4O_4$: 467.2629, found: 467.2623.

(3*S*,9*S*,15*S*)-3-Benzyl-7-isobutyl-9,15-dimethyl-1,4,7,10-tetraza-2,5,8,11-cyclopentadecanetetrone (Nleu-5S). ^{1}H NMR (400 MHz, MeOD): δ 7.32−7.15 (5H, m), 4.57 (1H, q, J = 7.2 Hz), 4.44 (1H, dd, J = 11.7, 3.6 Hz), 4.07 (1H, d, J = 14.7 Hz), 3.84−3.71 (1H, m), 3.65−3.54 (1H, m), 3.42 (1H, dd, J = 14.4, 3.6 Hz), 3.24−3.15 (1H, m), 2.94 (1H, dd, J = 14.2, 11.6 Hz), 2.15−2.04 (2H, m), 1.94−1.80 (2H, m), 1.75−1.51 (2H, m), 1.45−1.35 (1H, m), 1.32 (3H, d, J = 7.2 Hz), 1.15 (3H, d, J = 6.5 Hz), 0.97 (3H, d, J = 6.5 Hz), 0.89 (3H, d, J = 6.7 Hz); ^{13}C NMR (100 MHz, MeOD): δ 177.8, 177.2, 173.2, 171.7, 139.8, 130.1, 129.6, 127.7, 59.2, 57.1, 53.9, 47.8, 47.6, 37.2, 36.0, 35.6, 29.7, 24.8, 22.9, 20.61, 20.57, 16.6; HRMS [M + Na]$^+$ calcd for $C_{23}H_{34}N_4O_4$: 467.2629, found: 467.2621.

(3*S*,6*S*,15*R*)-3-Benzyl-6-isobutyl-10-methyl-15-methyl-1,4,7,10-tetraza-2,5,8,11-cyclopentadecanetetrone (Nala-5R). ^{1}H NMR (400 MHz, MeOD): δ 7.33−7.15 (5H, m), 4.57 (1H, dd, J = 11.8, 3.9 Hz), 4.10−4.02 (1H, m), 3.89−3.76 (2H, m), 3.47 (1H, dd, J = 14.4, 3.9 Hz), 2.98 (1H, dd, J = 15.3, 11.7 Hz), 2.22 (1H, dt, J = 13.3, 3.8 Hz), 2.05 (1H, td, J = 13.3, 3.4 Hz), 1.74−1.61 (2H, m), 1.58−1.41 (3H, m), 1.53 (3H, d, J = 7.2 Hz), 1.41−1.28 (2H, m), 1.10 (3H, d, J = 6.5 Hz), 0.87 (3H, d, J = 6.3 Hz), 0.82 (3H, d, J = 6.5 Hz); ^{13}C NMR (100 MHz, MeOD): δ 177.3, 174.8, 174.4, 173.0, 139.4, 130.4, 130.2, 129.7, 129.6, 127.8, 55.9, 55.0, 54.7, 47.2, 40.8, 39.9, 38.7, 35.7, 31.9, 25.9, 23.4, 23.3, 22.0, 21.6; HRMS [M + Na]$^+$ calcd for $C_{23}H_{34}N_4O_4$: 467.2629, found: 467.2628.

(3*S*,6*S*,15*S*)-3-Benzyl-6-isobutyl-10-methyl-15-methyl-1,4,7,10-tetraza-2,5,8,11-cyclopentadecanetetrone (Nala-5S). ^{1}H NMR (300 MHz, MeOD): δ 4.34−4.14 (5H, m), 4.70−4.60 (1H, m), 4.39−4.23 (1H, m), 4.14−3.90 (1H, m), 3.55 (1H, d, J = 15.0 Hz), 3.25−3.13 (3H, m), 2.99−2.86 (1H, dd, J = 13.5, 10.6 Hz), 2.64−1.75 (4H, m), 1.74−1.25 (6H, m), 1.25−1.12 (3H, m), 0.92−0.74 (6H, m); ^{13}C NMR (75 MHz, MeOD): δ 175.2, 171.9, 137.0, 128.8, 128.1, 126.4, 55.6, 53.5, 52.8, 46.1, 39.5, 38.6, 37.3, 34.4, 32.9, 31.1, 24.4, 24.3, 22.0, 21.6, 19.9, 17.1, 17.0; HRMS [M + Na]$^+$ calcd for $C_{23}H_{34}N_4O_4$: 467.2629, found: 467.2629.

(3*S*,6*S*)-3-Benzyl-10-isobutyl-6-methyl-1,4,7,10-tetraazacyclopentadecane-2,5,8,11-tetraone (32). ^{1}H NMR (400 MHz, DMSO-d_6): δ 8.89 (0.6H, d, J = 5.3 Hz, H_N Ala), 8.77 (0.4H, d, J = 5.6 Hz, H_N Ala), 8.48 (0.4H, br s), 8.42 (0.4H, d, J = 9.1 Hz, H_N Phe), 7.45−7.40 (0.4H, m, H_N Linker), 7.37 (0.6H, d, J = 9.6 Hz, H_N Phe), 7.31−7.12 (5H, m), 6.47 (0.6H, d, J = 8.5 Hz, H_N Linker), 6.30 (0.2H, br s), 4.45−4.28 (1H, m, H_α Phe), 4.16 (1H, d, J = 14.7 Hz, H_α Nleu), 3.93−3.76 (1H, m, H_α Ala), 3.62 (1H, d, J = 14.7 Hz, H_α Nleu), 3.66−3.58 (2H, m), 3.25−3.17 (1H, m, H_5 Linker), 3.16−3.08 (1H, m, H_β Phe), 2.99−2.90 (1H, ddd, J = 9.9, 6.8, 3.2 Hz, H_β Phe), 2.87−2.75 (1H, m, H_5 Linker), 2.74−2.65 (1H, m), 2.41−2.29 (0.4H, m), 2.04−1.95 (0.6H, dt, J = 14.3, 3.4 Hz), 1.89−1.69 (1H, m, H_γ Nleu), 1.64−1.34 (2H, m, H_4 Linker), 1.16−1.04 (1H, m), 1.00 (1H, d, J = 7.3 Hz,

https://doi.org/10.1021/acs.jmedchem.0c02036
J. Med. Chem. 2021, 64, 5365−5383

H_β Ala), 0.92 (1.5H, d, J = 6.7 Hz, H_δ Leu), 0.87 (1.5H, d, J = 6.7 Hz, H_δ Leu), 0.82 (1.5H, d, J = 6.7 Hz, H_δ Leu), 0.75 (1.5H, d, J = 6.7 Hz, H_δ Leu). HRMS $[M + Na]^+$ calcd for $C_{23}H_{34}N_4O_4$: 453.2472, found: 453.2472.

(3*S*,9*S*)-3-Benzyl-9-isobutyl-7-methyl-1,4,7,10-tetraazacyclopentadecane-2,5,8,11-tetraone (33). ^{1}H NMR (400 MHz, DMSO-d_6): δ 8.32 (1H, d, J = 8.4 Hz, H_N Phe), 7.92 (1H, d, J = 8.4 Hz, H_N Leu), 7.37 (1H, t, J = 5.6 Hz, H_N Linker), 7.31−7.14 (5H, m), 4.75−4.62 (1H, m, H_α Leu), 4.29 (1H, d, J = 14.2 Hz, H_α Nala), 4.27−4.21 (1H, m, H_α Phe), 3.21 (1H, d, J = 14.0 Hz, H_α Nala), 3.17−3.10 (1H, m, H_β Phe), 3.13 (3H, s, H_β Nala), 3.04 (1H, q, J = 5.8 Hz, H_5 Linker), 2.73 (1H, dd, J = 14.0, 10.3 Hz), 2.22 (1H, ddd, J = 12.6, 9.7, 4.7 Hz, H_2 Linker), 1.95−1.87 (1H, m, H_2 Linker), 1.68−1.54 (2H, m, H_4 Linker and H_γ Leu), 1.53−1.32 (4H, m, H_β Leu), 1.26−1.13 (1H, m, H_4 Linker), 0.89 (6H, dd, J = 6.5, 5.5 Hz, H_δ Leu). HRMS $[M + Na]^+$ calcd for $C_{23}H_{34}N_4O_4$: 453.2472, found: 453.2470.

(3*S*,6*S*,9*S*,12*S*)-3-Benzyl-6-isobutyl-7,9,12-trimethyl-1,4,7,10-tetraazacyclopentadecane-2,5,8,11-tetraone (NMe-Leu-2S). ^{1}H NMR (400 MHz, DMSO-d_6): δ 8.06 (dd, J = 32.5, 7.7 Hz, 1H), 7.70 (dd, J = 17.3, 8.5 Hz, 1H), 7.56 (dd, J = 7.9, 3.5 Hz, 1H), 7.30−7.15 (m, 5H), 4.66−4.52 (m, 2H), 4.11−4.04 (m, 1H), 3.23−3.07 (m, 3H), 2.88 (d, J = 10.2 Hz, 2H), 2.28 (s, 2H), 2.11 (s, 1H), 1.84−1.69 (m, 1H), 1.63−1.53 (m, 1H), 1.46−1.31 (m, 2H) 1.28−1.19 (m, 2H), 1.14 (dd, J = 14.8, 6.8 Hz, 3H), 0.98 (d, J = 6.1 Hz, 1H), 0.93 (d, J = 6.7 Hz, 3H), 0.86 (d, J = 6.4 Hz, 3H), 0.83 (d, J = 6.6 Hz, 3H). ^{13}C NMR (101 MHz, DMSO): δ 175.4, 171.7, 170.6, 169.4, 137.8, 129.0, 128.2, 126.4, 58.6, 54.3, 44.4, 37.4, 36.5, 36.2, 35.6, 30.0, 28.5, 24.3, 23.1, 21.8, 18.0, 15.8. HRMS $[M + Na]^+$ calcd for $C_{25}H_{38}N_4O_4$: 481.2785, found: 481.2797.

(3*S*,6*S*,9*S*,12*S*)-3-Benzyl-6-isobutyl-6,9,12-trimethyl-1,4,7,10-tetraazacyclopentadecane-2,5,8,11-tetraone (αMe-Leu-2S). ^{1}H NMR (400 MHz, DMSO-d_6): δ 8.52 (s, 1H), 8.34 (d, J = 5.2 Hz, 1H), 7.31−7.14 (m, 6H), 6.87 (dd, J = 8.8, 2.0 Hz, 1H), 4.03 (dd, J = 7.2, 5.3 Hz, 1H), 3.82−3.76 (m, 1H), 3.41−3.37 (m, 1H), 3.29−3.24 (m, 2H), 2.79 (dd, J = 13.6, 2.7 Hz, 1H), 2.32−2.23 (m, 1H), 1.96 (d, J = 6.8 Hz, 1H), 1.66−1.42 (m, 4H), 1.32 (d, J = 8.8 Hz, 1H), 1.17 (d, J = 7.1 Hz, 3H), 1.13−1.07 (m, 1H), 0.96 (s, 3H), 0.88 (d, J = 6.7 Hz, 3H), 0.84 (d, J = 6.6 Hz, 3H), 0.79 (d, J = 6.6 Hz, 3H). ^{13}C NMR (101 MHz, DMSO): δ 176.6, 174.5, 174.3, 170.3, 139.5, 129.1, 128.0, 126.0, 59.1, 57.7, 49.4, 38.0, 33.5, 30.2, 25.2, 24.8, 23.8, 23.5, 23.3, 17.7, 15.9. HRMS $[M + Na]^+$ calcd for $C_{25}H_{38}N_4O_4$: 481.2785, found: 481.2790.

(3*S*,6*R*,9*S*,12*S*)-3-Benzyl-6-isobutyl-7,9,12-trimethyl-1,4,7,10-tetraazacyclopentadecane-2,5,8,11-tetraone ((D)-NMeLeu-2S). ^{1}H NMR (400 MHz, DMSO-d_6): δ 8.02 (d, J = 9.1 Hz, 1H), 7.83 (d, J = 8.3 Hz, 1H), 7.63 (t, J = 5.8 Hz, 1H), 7.33−7.11 (m, 5H), 4.76 (dd, J = 8.3, 6.8 Hz, 2H), 4.43 (td, J = 9.6, 5.1 Hz, 1H), 3.25−3.15 (m, 1H), 3.04 (dd, J = 13.7, 5.1 Hz, 1H), 2.94−2.86 (m, 1H), 2.83 (s, 3H), 2.72 (dd, J = 13.7, 10.0 Hz, 1H), 2.35 (q, J = 6.5 Hz, 1H), 1.46 (ddd, J = 13.4, 8.4, 6.7 Hz, 2H), 1.37−1.19 (m, 3H), 1.15 (d, J = 6.7 Hz, 3H), 1.13−1.06 (m, 1H), 1.03−0.97 (m, 1H), 0.92 (d, J = 6.6 Hz, 3H), 0.82 (d, J = 6.5 Hz, 3H), 0.72 (d, J = 6.5 Hz, 3H). ^{13}C NMR (101 MHz, DMSO): δ 175.0, 173.6, 171.1, 169.9, 138.2, 129.0, 128.0, 126.1, 54.4, 54.2, 44.2, 37.4, 37.0, 36.1, 31.4, 29.9, 26.1, 24.1, 22.6, 22.3, 17.5, 15.9. HRMS $[M + Na]^+$ calcd for $C_{25}H_{38}N_4O_4$: 481.2785, found: 481.2793.

(3*S*,6*R*,9*S*,12*S*)-3-Benzyl-6-isobutyl-9,12-dimethyl-1,4,7,10-tetraazacyclopentadecane-2,5,8,11-tetraone ((D)Leu-2S). ^{1}H NMR (400 MHz, DMSO-d_6): δ 8.63−8.42 (m, 2H), 8.01 (dd, J = 21.2, 7.6 Hz, 1H), 7.73 (d, J = 7.7 Hz, 1H), 7.27−7.14 (m, 6H), 4.36−4.31 (m, 1H), 4.28−4.22 (m, 1H), 4.18−4.12 (m, 1H), 4.08−4.01 (m, 1H), 3.92−3.83 (m, 1H), 3.17 (ddd, J = 13.8, 3.8, 1.8 Hz, 1H), 2.76−2.65 (m, 2H), 2.37−2.29 (m, 1H), 2.15 (d, J = 3.8 Hz, 1H), 1.61 (s, 1H), 1.30−1.20 (m, 4H), 1.15 (d, J = 7.1 Hz, 2H), 1.05−0.97 (m, 3H), 0.77 (d, J = 6.4 Hz, 3H), 0.68 (t, J = 6.2 Hz, 3H). ^{13}C NMR (101 MHz, DMSO): δ 175.6, 174.5, 171.7, 170.8, 129.0, 128.0, 127.9, 126.0, 48.2, 38.1, 26.1, 23.9, 23.8, 22.9, 22.7, 22.2, 21.9, 17.4, 16.4, 16.0. HRMS $[M + Na]^+$ calcd for $C_{24}H_{36}N_4O_4$: 467.2629, found: 467.2630.

■ ASSOCIATED CONTENT

Supporting Information

The Supporting Information is available free of charge at https://pubs.acs.org/doi/10.1021/acs.jmedchem.0c02036.

Detailed NMR analysis of Nleu-2R, Nleu-2S, Nleu-5R, and Nleu-5S; analysis of MD simulations; permeability data; and NMR spectra (PDF)

SMILES, molecular formula strings, and all permeability data (CSV)

■ AUTHOR INFORMATION

Corresponding Authors

Philippe Sarret − *Département de Pharmacologie−Physiologie, Institut de Pharmacologie de Sherbrooke, Université de Sherbrooke, Sherbrooke, Quebec, Canada J1H5N4*; orcid.org/0000-0002-7627-701X; Email: Philippe.Sarret.@USherbrooke.ca

Sereina Riniker − *Department of Chemistry and Applied Biosciences, ETH Zürich, 8093 Zürich, Switzerland*; orcid.org/0000-0003-1893-4031; Email: sriniker@ethz.ch

Authors

Christian Comeau − *Département de Pharmacologie−Physiologie, Institut de Pharmacologie de Sherbrooke, Université de Sherbrooke, Sherbrooke, Quebec, Canada J1H5N4*

Benjamin Ries − *Department of Chemistry and Applied Biosciences, ETH Zürich, 8093 Zürich, Switzerland*; orcid.org/0000-0002-0945-8304

Thomas Stadelmann − *Department of Chemistry and Applied Biosciences, ETH Zürich, 8093 Zürich, Switzerland*; orcid.org/0000-0003-2919-0939

Jacob Tremblay − *Département de Pharmacologie−Physiologie, Institut de Pharmacologie de Sherbrooke, Université de Sherbrooke, Sherbrooke, Quebec, Canada J1H5N4*

Sylvain Poulet − *Département de Pharmacologie−Physiologie, Institut de Pharmacologie de Sherbrooke, Université de Sherbrooke, Sherbrooke, Quebec, Canada J1H5N4*

Ulrike Fröhlich − *Département de Pharmacologie−Physiologie, Institut de Pharmacologie de Sherbrooke, Université de Sherbrooke, Sherbrooke, Quebec, Canada J1H5N4*

Jérôme Côté − *Département de Pharmacologie−Physiologie, Institut de Pharmacologie de Sherbrooke, Université de Sherbrooke, Sherbrooke, Quebec, Canada J1H5N4*

Pierre-Luc Boudreault − *Département de Pharmacologie−Physiologie, Institut de Pharmacologie de Sherbrooke, Université de Sherbrooke, Sherbrooke, Quebec, Canada J1H5N4*

Rabeb Mouna Derbali − *Faculté de pharmacie, Université de Montréal, Montréal, Quebec, Canada H3C 3J7*

Michel Grandbois − *Département de Pharmacologie−Physiologie, Institut de Pharmacologie de Sherbrooke, Université de Sherbrooke, Sherbrooke, Quebec, Canada J1H5N4*

Grégoire Leclair − *Faculté de pharmacie, Université de Montréal, Montréal, Quebec, Canada H3C 3J7*

Éric Marsault − *Département de Pharmacologie−Physiologie, Institut de Pharmacologie de Sherbrooke, Université de Sherbrooke, Sherbrooke, Quebec, Canada J1H5N4*; orcid.org/0000-0002-5305-8762

Complete contact information is available at:
https://pubs.acs.org/10.1021/acs.jmedchem.0c02036

Author Contributions

[⊥]C.C. and B.R. contributed equally to this work.

Funding

Financial support from the Natural Sciences and Engineering Research Council of Canada, the Canada Foundation for Innovation, the Centre des Neurosciences de Sherbrooke, the Swiss National Science Foundation (grant no. 20002-178762), and ETH Zurich (ETH-34 17-2) is gratefully acknowledged.

Notes

The authors declare no competing financial interest.

■ ACKNOWLEDGMENTS

M. M. Gregor Weiss and Shuzhe Wang are acknowledged for helpful discussions.

■ DEDICATION

[‖]This article is dedicated to our close colleague, best friend, and research director, Prof. Éric Marsault, who passed away far too early.

■ ABBREVIATIONS

ACN, acetonitrile; DEPBT, (3-(diethoxyphosphoryloxy)-1,2,3-benzotriazin-4(3H)-one); DIBAL, diisobutylaluminium hydride; DIC, *N,N′*-diisopropylcarbodiimide; DIPEA, N,N-diisopropylethylamine; DPPA, diphenylphosphoryl azide; EXSY, exchange spectroscopy; KHMDS, potassium bis-(trimethylsilyl)amide; Nala, alanine peptoid (N-methylglycine); Nleu, leucine peptoid (N-isobutylglycine); Nphe, phenylalanine peptoid (N-benzylglycine); PDC, pyridinium dichromate

■ REFERENCES

(1) Driggers, E. M.; Hale, S. P.; Lee, J.; Terrett, N. K. The Exploration of Macrocycles for Drug Discovery–an Underexploited Structural Class. *Nat. Rev. Drug Discovery* **2008**, *7*, 608−624.
(2) Mallinson, J.; Collins, I. Macrocycles in New Drug Discovery. *Future Med. Chem.* **2012**, *4*, 1409−1438.
(3) Dougherty, P. G.; Qian, Z.; Pei, D. Macrocycles as Protein−Protein Interaction Inhibitors. *Biochem. J.* **2017**, 1109−1125.
(4) Marsault, E.; Peterson, M. L. Macrocycles Are Great Cycles: Applications, Opportunities, and Challenges of Synthetic Macrocycles in Drug Discovery. *J. Med. Chem.* **2011**, *54*, 1961−2004.
(5) Abdalla, M. A.; McGaw, L. J. Natural Cyclic Peptides as an Attractive Modality for Therapeutics: A Mini Review. *Molecules* **2018**, No. 2080.
(6) Marsault, E.; Peterson, M. L., Eds.; *Practical Medicinal Chemistry with Macrocycles*; John Wiley & Sons, Inc.: Hoboken, NJ, 2017.
(7) Janin, J.; Bahadur, R. P.; Chakrabarti, P. Protein-Protein Interaction and Quaternary Structure. *Q. Rev. Biophys.* **2008**, *41*, 133−180.
(8) Chène, P. Drugs Targeting Protein-Protein Interactions. *ChemMedChem* **2006**, *1*, 400−411.
(9) Scott, D. E.; Bayly, A. R.; Abell, C.; Skidmore, J. Small Molecules, Big Targets: Drug Discovery Faces the Protein-Protein Interaction Challenge. *Nat. Rev. Drug Discovery* **2016**, *15*, 533−550.
(10) Modell, A. E.; Blosser, S. L.; Arora, P. S. Systematic Targeting of Protein-Protein Interactions Approaches to Targeting Protein-Protein Interactions. *Trends Pharmacol. Sci.* **2016**, *37*, 702−713.
(11) Giordanetto, F.; Kihlberg, J. Macrocyclic Drugs and Clinical Candidates: What Can Medicinal Chemists Learn from Their Properties? *J. Med. Chem.* **2014**, *57*, 278−295.
(12) Naylor, M. R.; Bockus, A. T.; Blanco, M. J.; Lokey, R. S. Cyclic Peptide Natural Products Chart the Frontier of Oral Bioavailability in the Pursuit of Undruggable Targets. *Curr. Opin. Chem. Biol.* **2017**, *38*, 141−147.
(13) Fosgerau, K.; Hoffmann, T. Peptide Therapeutics: Current Status and Future Directions. *Drug Discovery Today* **2015**, *20*, 122−128.
(14) Wang, C. K.; Northfield, S. E.; Colless, B.; Chaousis, S.; Hamernig, I.; Lohman, R.-J.; Nielsen, D. S.; Schroeder, C. I.; Liras, S.; Price, D. A.; Fairlie, D. P.; Craik, D. J. Rational Design and Synthesis of an Orally Bioavailable Peptide Guided by NMR Amide Temperature Coefficients. *Proc. Natl. Acad. Sci. U.S.A.* **2014**, *111*, 17504−17509.
(15) Nielsen, D. S.; Hoang, H. N.; Lohman, R. J.; Hill, T. A.; Lucke, A. J.; Craik, D. J.; Edmonds, D. J.; Griffith, D. A.; Rotter, C. J.; Ruggeri, R. B.; Price, D. A.; Liras, S.; Fairlie, D. P. Improving on Nature: Making a Cyclic Heptapeptide Orally Bioavailable. *Angew. Chem., Int. Ed.* **2014**, *53*, 12059−12063.
(16) Whitty, A.; Zhong, M.; Viarengo, L.; Beglov, D.; Hall, D. R.; Vajda, S. Quantifying the Chameleonic Properties of Macrocycles and Other High-Molecular-Weight Drugs. *Drug Discovery Today* **2016**, 712.
(17) Danelius, E.; Poongavanam, V.; Peintner, S.; Wieske, L. H. E.; Erdélyi, M.; Kihlberg, J. Solution Conformations Explain the Chameleonic Behaviour of Macrocyclic Drugs. *Chem. − Eur. J.* **2020**, *26*, 5231−5244.
(18) Witek, J.; Mühlbauer, M.; Keller, B. G.; Blatter, M.; Meissner, A.; Wagner, T.; Riniker, S. Interconversion Rates between Conformational States as Rationale for the Membrane Permeability of Cyclosporines. *ChemPhysChem* **2017**, *18*, 3309−3314.
(19) Räder, A. F. B.; Reichart, F.; Weinmüller, M.; Kessler, H. Improving Oral Bioavailability of Cyclic Peptides by N-Methylation. *Bioorg. Med. Chem.* **2018**, *26*, 2766−2773.
(20) White, T. R.; Renzelman, C. M.; Rand, A. C.; Rezai, T.; McEwen, C. M.; Gelev, V. M.; Turner, R. A.; Linington, R. G.; Leung, S. S. F.; Kalgutkar, A. S.; Bauman, J. N.; Zhang, Y.; Liras, S.; Price, D. A.; Mathiowetz, A. M.; Jacobson, M. P.; Lokey, R. S. On-Resin N-Methylation of Cyclic Peptides for Discovery of Orally Bioavailable Scaffolds. *Nat. Chem. Biol.* **2011**, *7*, 810−817.
(21) Beck, J. G.; Chatterjee, J.; Laufer, B.; Kiran, M. U.; Frank, A. O.; Neubauer, S.; Ovadia, O.; Greenberg, S.; Gilon, C.; Hoffman, A.; Kessler, H. Intestinal Permeability of Cyclic Peptides: Common Key Backbone Motifs Identified. *J. Am. Chem. Soc.* **2012**, *134*, 12125−12133.
(22) Biron, E.; Chatterjee, J.; Ovadia, O.; Langenegger, D.; Brueggen, J.; Hoyer, D.; Schmid, H. A.; Jelinek, R.; Gilon, C.; Hoffman, A.; Kessler, H. Improving Oral Bioavailability of Peptides by Multiple N-Methylation: Somatostatin Analogues. *Angew. Chem., Int. Ed.* **2008**, *47*, 2595−2599.
(23) White, T. R.; Renzelman, C. M.; Rand, A. C.; Rezai, T.; Mcewen, C. M.; Gelev, V. M.; Turner, R. A.; Linington, R. G.; Leung, S. S. F.; Amit, S. On-Resin N-Methylation of Cyclic Peptides for Discovery of Orally Bioavailable Scaffolds. *Nat. Chem. Biol.* **2011**, *7*, 810−817.
(24) Schwochert, J.; Turner, R.; Thang, M.; Berkeley, R. F.; Ponkey, A. R.; Rodriguez, K. M.; Leung, S. S. F.; Khunte, B.; Goetz, G.; Limberakis, C.; Kalgutkar, A. S.; Eng, H.; Shapiro, M. J.; Mathiowetz, A. M.; Price, D. A.; Liras, S.; Jacobson, M. P.; Lokey, R. S. Peptide to Peptoid Substitutions Increase Cell Permeability in Cyclic Hexapeptides. *Org. Lett.* **2015**, *17*, 2928−2931.
(25) Sui, Q.; Borchardt, D.; Rabenstein, D. L. Kinetics and Equilibria of Cis/Trans Isomerization of Backbone Amide Bonds in Peptoids. *J. Am. Chem. Soc.* **2007**, *129*, 12042−12048.
(26) Culf, A. S.; Ouellette, R. J. Solid-Phase Synthesis of N-Substituted Glycine Oligomers (α-Peptoids) and Derivatives. *Molecules* **2010**, *15*, 5282−5335.
(27) Riniker, S. Toward the Elucidation of the Mechanism for Passive Membrane Permeability of Cyclic Peptides. *Future Med. Chem.* **2019**, *11*, 637−639.
(28) Witek, J.; Wang, S.; Schroeder, B.; Lingwood, R.; Dounas, A.; Roth, H. J.; Fouché, M.; Blatter, M.; Lemke, O.; Keller, B.; Riniker, S. Rationalization of the Membrane Permeability Differences in a Series of Analogue Cyclic Decapeptides. *J. Chem. Inf. Model.* **2019**, *59*, 294−308.

(29) Marsault, E.; Benakli, K.; Beaubien, S.; Saint-Louis, C.; Déziel, R.; Fraser, G. Potent Macrocyclic Antagonists to the Motilin Receptor Presenting Novel Unnatural Amino Acids. *Bioorg. Med. Chem. Lett.* **2007**, *17*, 4187−4190.
(30) Hoveyda, H. R.; Marsault, E.; Gagnon, R.; Mathieu, A. P.; Vézina, M.; Landry, A.; Wang, Z.; Benakli, K.; Beaubien, S.; Saint-Louis, C.; Brassard, M.; Pinault, J. F.; Ouellet, L.; Bhat, S.; Ramaseshan, M.; Peng, X.; Foucher, L.; Beauchemin, S.; Bhérer, P.; Veber, D. F.; Peterson, M. L.; Fraser, G. L. Optimization of the Potency and Pharmacokinetic Properties of a Macrocyclic Ghrelin Receptor Agonist (Part I): Development of Ulimorelin (TZP-101) from Hit to Clinic. *J. Med. Chem.* **2011**, *54*, 8305−8320.
(31) Le Roux, A.; Blaise, E.; Boudreault, P.-L.; Comeau, C.; Doucet, A.; Giarrusso, M.; Collin, M.-P.; Neubauer, T.; Koelling, F.; Göller, A. H.; Seep, L.; Tshitenge, D. T.; Wittwer, M.; Kullmann, M.; Hillisch, A.; Mittendorf, J.; Marsault, É. Structure-Permeability Relationship of Semi-Peptidic Macrocycles − Understanding and Optimizing Passive Permeability and Efflux Ratio. *J. Med. Chem.* **2020**, 6774.
(32) Appavoo, S. D.; Huh, S.; Diaz, D. B.; Yudin, A. K. Conformational Control of Macrocycles by Remote Structural Modification. *Chem. Rev.* **2019**, 9724.
(33) Bockus, A. T.; Schwochert, J. A.; Pye, C. R.; Townsend, C. E.; Sok, V.; Bednarek, M. A.; Lokey, R. S. Going Out on a Limb: Delineating the Effects of β-Branching, N-Methylation, and Side Chain Size on the Passive Permeability, Solubility, and Flexibility of Sanguinamide A Analogues. *J. Med. Chem.* **2015**, *58*, 7409−7418.
(34) Hewitt, W. M.; Leung, S. S. F.; Pye, C. R.; Ponkey, A. R.; Bednarek, M.; Jacobson, M. P.; Lokey, R. S. Cell-Permeable Cyclic Peptides from Synthetic Libraries Inspired by Natural Products. *J. Am. Chem. Soc.* **2015**, *137*, 715−721.
(35) Rezai, T.; Yu, B.; Millhauser, G. L.; Jacobson, M. P.; Lokey, R. S. Testing the Conformational Hypothesis of Passive Membrane Permeability Using Synthetic Cyclic Peptide Diastereomers. *J. Am. Chem. Soc.* **2006**, *128*, 2510−2511.
(36) Over, B.; Matsson, P.; Tyrchan, C.; Artursson, P.; Doak, B. C.; Foley, M. A.; Hilgendorf, C.; Johnston, S. E.; Lee, M. D.; Lewis, R. J.; McCarren, P.; Muncipinto, G.; Norinder, U.; Perry, M. W. D.; Duvall, J. R.; Kihlberg, J. Structural and Conformational Determinants of Macrocycle Cell Permeability. *Nat. Chem. Biol.* **2016**, 1065.
(37) Di, L.; Kerns, E. H. *Drug-Like Properties*, 2nd ed.; Elsevier, 2016.
(38) Balazs, A. Y. S.; Carbajo, R. J.; Davies, N. L.; Dong, Y.; Hird, A. W.; Johannes, J. W.; Lamb, M. L.; McCoull, W.; Raubo, P.; Robb, G. R.; Packer, M. J.; Chiarparin, E. Free Ligand 1D NMR Conformational Signatures to Enhance Structure Based Drug Design of a Mcl-1 Inhibitor (AZD5991) and Other Synthetic Macrocycles. *J. Med. Chem.* **2019**, *62*, 9418−9437.
(39) Orwig, K. S.; Dix, T. A. Synthesis of Cα Methylated Carboxylic Acids: Isosteres of Arginine and Lysine for Use as N-Terminal Capping Residues in Polypeptides. *Tetrahedron Lett.* **2005**, *46*, 7007−7009.
(40) Lebel, H.; Leogane, O. Boc-Protected Amines via a Mild and Efficient One-Pot Curtius Rearrangement. *Org. Lett.* **2005**, *7*, 4107−4110.
(41) Ye, T.; McKervey, M. A. Organic Synthesis with α-Diazocarbonyl Compounds. *Chem. Rev.* **1994**, *94*, 1091−1160.
(42) Kerns, E. H.; Di, L.; Petusky, S.; Farris, M.; Ley, R.; Jupp, P. Combined Application of Parallel Artificial Membrane Permeability Assay and Caco-2 Permeability Assays in Drug Discovery. *J. Pharm. Sci.* **2004**, *93*, 1440−1453.
(43) Laursen, J. S.; Engel-Andreasen, J.; Fristrup, P.; Harris, P.; Olsen, C. A. Cis-Trans Amide Bond Rotamers in β-Peptoids and Peptoids: Evaluation of Stereoelectronic Effects in Backbone and Side Chains. *J. Am. Chem. Soc.* **2013**, *135*, 2835−2844.
(44) Engel-Andreasen, J.; Wich, K.; Laursen, J. S.; Harris, P.; Olsen, C. A. Effects of Thionation and Fluorination on Cis-Trans Isomerization in Tertiary Amides: An Investigation of N-Alkylglycine (Peptoid) Rotamers. *J. Org. Chem.* **2015**, *80*, 5415−5427.
(45) Sebastiano, M. R.; Doak, B. C.; Backlund, M.; Poongavanam, V.; Over, B.; Ermondi, G.; Caron, G.; Kihlberg, J. Impact of Dynamically Exposed Polarity on Permeability and Solubility of Chameleonic Drugs Beyond the Rule of 5. *J. Med. Chem.* **2018**, 4189.
(46) Alex, A.; Millan, D. S.; Perez, M.; Wakenhut, F.; Whitlock, G. A. Intramolecular Hydrogen Bonding to Improve Membrane Permeability and Absorption in beyond Rule of Five Chemical Space. *MedChemComm* **2011**, *2*, 669−674.
(47) Tyagi, M.; Poongavanam, V.; Lindhagen, M.; Pettersen, A.; Sjö, P.; Schiesser, S.; Kihlberg, J. Toward the Design of Molecular Chameleons: Flexible Shielding of an Amide Bond Enhances Macrocycle Cell Permeability. *Org. Lett.* **2018**, *20*, 5737−5742.
(48) Shapiro, S. S.; Wilk, M. B. Biometrika Trust An Analysis of Variance Test for Normality (Complete Samples) Published by: Oxford University Press on Behalf of Biometrika Trust Stable. *Biometrika* **1965**, *52*, 591−611.
(49) Kotz, S.; Johnson, N. L. Breakthroughs in Statistics, Volume III. *Technometrics* **1998**, *40*, 165.
(50) Vorherr, T.; Lewis, I.; Berghausen, J.; Desrayaud, S.; Schaefer, M. Modulation of Oral Bioavailability and Metabolism for Closely Related Cyclic Hexapeptides. *Int. J. Pept. Res. Ther.* **2018**, *24*, 35−48.
(51) Peraro, L.; Kritzer, J. A. Emerging Methods and Design Principles for Cell-Penetrant Peptides. *Angew. Chem., Int. Ed.* **2018**, *57*, 11868−11881.
(52) Schrödinger, L. *The PyMOL Molecular Graphics System*, version 1.8; Schrödinger, LLC, 2015.
(53) Kansy, M.; Senner, F.; Gubernator, K. Physicochemical High Throughput Screening: Parallel Artificial Membrane Permeation Assay in the Description of Passive Absorption Processes. *J. Med. Chem.* **1998**, *41*, 1007−1010.
(54) Avdeef, A. *Absorption and Drug Development*; John Wiley & Sons, Inc.: Hoboken, NJ, 2012.
(55) Hidalgo, I. J.; Raub, T. J.; Borchardt, R. T. Characterization of the Human Colon Carcinoma Cell Line (Caco-2) as a Model System for Intestinal Epithelial Permeability. *Gastroenterology* **1989**, *96*, 736−749.
(56) Hubatsch, I.; Ragnarsson, E. G. E.; Artursson, P. Determination of Drug Permeability and Prediction of Drug Absorption in Caco-2 Monolayers. *Nat. Protoc.* **2007**, *2*, 2111−2119.
(57) Hawkins, P. C. D.; Nicholls, A. Conformer Generation with OMEGA: Learning from the Data Set and the Analysis of Failures. *J. Chem. Inf. Model.* **2012**, *52*, 2919−2936.
(58) Hawkins, P. C. D.; Skillman, A. G.; Warren, G. L.; Ellingson, B. A.; Stahl, M. T. Conformer Generation with OMEGA: Algorithm and Validation Using High Quality Structures from the Protein Databank and Cambridge Structural Database. *J. Chem. Inf. Model.* **2010**, *50*, 572−584.
(59) Poongavanam, V.; Danelius, E.; Peintner, S.; Alcaraz, L.; Caron, G.; Cummings, M. D.; Wlodek, S.; Erdelyi, M.; Hawkins, P. C. D.; Ermondi, G.; Kihlberg, J. Conformational Sampling of Macrocyclic Drugs in Different Environments: Can We Find the Relevant Conformations? *ACS Omega* **2018**, *3*, 11742−11757.
(60) Ruder, S. An Overview of Gradient Descent Optimization Algorithms. 2016, arXiv:1609.04747. arXiv.org e-Print archive. https://arxiv.org/abs/1609.04747.
(61) Schmid, N.; Christ, C. D.; Christen, M.; Eichenberger, A. P.; Van Gunsteren, W. F. Architecture, Implementation and Parallelisation of the GROMOS Software for Biomolecular Simulation. *Comput. Phys. Commun.* **2012**, *183*, 890−903.
(62) Schmid, N.; Eichenberger, A. P.; Choutko, A.; Riniker, S.; Winger, M.; Mark, A. E.; Van Gunsteren, W. F. Definition and Testing of the GROMOS Force-Field Versions 54A7 and 54B7. *Eur. Biophys. J.* **2011**, *40*, 843−856.
(63) Berendsen, H. J. C.; Postma, J. P.; van Gunsteren, W. F.; Hermans, J. Interaction Models for Water in Relation to Protein Hydration. In *Intermolecular Forces*; Pullman, B., Ed.; Springer, 1981; Vol. *14*, pp 331−342.
(64) Tironi, I. G.; Van Gunsteren, W. F. A Molecular Dynamics Simulation Study of Chloroform. *Mol. Phys.* **1994**, *83*, 381−403.
(65) Van Gunsteren, W. F.; Berendsen, H. J. C. A Leap-Frog Algorithm for Stochastic Dynamics. *Mol. Simul.* **1988**, *1*, 173−185.

https://doi.org/10.1021/acs.jmedchem.0c02036
J. Med. Chem. 2021, 64, 5365−5383

(66) Ryckaert, J. P.; Ciccotti, G.; Berendsen, H. J. C. Numerical Integration of the Cartesian Equations of Motion of a System with Constraints: Molecular Dynamics of n-Alkanes. *J. Comput. Phys.* **1977**, *23*, 327−341.
(67) Tironi, I. G.; Sperb, R.; Smith, P. E.; van Gunsteren, W. F. A Generalized Reaction Field Method for Molecular Dynamics Simulations. *J. Chem. Phys.* **1995**, *102*, 5451−5459.
(68) Heinz, T. N.; Van Gunsteren, W. F.; Hünenberger, P. H. Comparison of Four Methods to Compute the Dielectric Permittivity of Liquids from Molecular Dynamics Simulations. *J. Chem. Phys.* **2001**, *115*, 1125−1136.
(69) Berendsen, H. J. C.; Postma, J. P. M.; van Gunsteren, W. F.; DiNola, A.; Haak, J. R. Molecular Dynamics with Coupling to an External Bath. *J. Chem. Phys.* **1984**, *81*, 3684−3690.
(70) Scherer, M. K.; Trendelkamp-Schroer, B.; Paul, F.; Pérez-Hernández, G.; Hoffmann, M.; Plattner, N.; Wehmeyer, C.; Prinz, J.-H.; Noé, F. PyEMMA 2: A Software Package for Estimation, Validation, and Analysis of Markov Models. *J. Chem. Theory Comput.* **2015**, *11*, 5525−5542.
(71) McGibbon, R. T.; Beauchamp, K. A.; Harrigan, M. P.; Klein, C.; Swails, J. M.; Hernández, C. X.; Schwantes, C. R.; Wang, L. P.; Lane, T. J.; Pande, V. S. MDTraj: A Modern Open Library for the Analysis of Molecular Dynamics Trajectories. *Biophys. J.* **2015**, *109*, 1528−1532.
(72) Molgedey, L.; Schuster, H. G. Separation of a Mixture of Independent Signals Using Time Delayed Correlations. *Phys. Rev. Lett.* **1994**, *72*, 3634−3637.
(73) Keller, B.; Daura, X.; Van Gunsteren, W. F. Comparing Geometric and Kinetic Cluster Algorithms for Molecular Simulation Data. *J. Chem. Phys.* **2010**, *132*, No. 074110.
(74) Weiß, R. G.; Ries, B.; Wang, S.; Riniker, S. Volume-Scaled Common Nearest Neighbor Clustering Algorithm with Free-Energy Hierarchy. *J. Chem. Phys.* **2021**, *154*, 084106.
(75) Eichenberger, A. P.; Allison, J. R.; Dolenc, J.; Geerke, D. P.; Horta, B. A. C.; Meier, K.; Oostenbrink, C.; Schmid, N.; Steiner, D.; Wang, D.; Van Gunsteren, W. F. GROMOS++ Software for the Analysis of Biomolecular Simulation Trajectories. *J. Chem. Theory Comput.* **2011**, *7*, 3379−3390.
(76) Vögeli, B.; Olsson, S.; Riek, R.; Güntert, P. Compiled Data Set of Exact NOE Distance Limits, Residual Dipolar Couplings and Scalar Couplings for the Protein GB3. *Data Brief* **2015**, *5*, 99−106.
(77) Virtanen, P.; Gommers, R.; Oliphant, T. E.; Haberland, M.; Reddy, T.; Cournapeau, D.; Burovski, E.; Peterson, P.; Weckesser, W.; Bright, J.; van der Walt, S. J.; Brett, M.; Wilson, J.; Millman, K. J.; Mayorov, N.; Nelson, A. R. J.; Jones, E.; Kern, R.; Larson, E.; Carey, C. J.; Polat, İ.; Feng, Y.; Moore, E. W.; VanderPlas, J.; Laxalde, D.; Perktold, J.; Cimrman, R.; Henriksen, I.; Quintero, E. A.; Harris, C. R.; Archibald, A. M.; Ribeiro, A. H.; Pedregosa, F.; van Mulbregt, P.; Vijaykumar, A.; Bardelli, A.; Pietro; Rothberg, A.; Hilboll, A.; Kloeckner, A.; Scopatz, A.; Lee, A.; Rokem, A.; Woods, C. N.; Fulton, C.; Masson, C.; Häggström, C.; Fitzgerald, C.; Nicholson, D. A.; Hagen, D. R.; Pasechnik, D. V.; Olivetti, E.; Martin, E.; Wieser, E.; Silva, F.; Lenders, F.; Wilhelm, F.; Young, G.; Price, G. A.; Ingold, G. L.; Allen, G. E.; Lee, G. R.; Audren, H.; Probst, I.; Dietrich, J. P.; Silterra, J.; Webber, J. T.; Slavi, J.; Nothman, J.; Buchner, J.; Kulick, J.; Schönberger, J. L.; de Miranda Cardoso, J. V.; Reimer, J.; Harrington, J.; Rodríguez, J. L. C.; Nunez-Iglesias, J.; Kuczynski, J.; Tritz, K.; Thoma, M.; Newville, M.; Kümmerer, M.; Bolingbroke, M.; Tartre, M.; Pak, M.; Smith, N. J.; Nowaczyk, N.; Shebanov, N.; Pavlyk, O.; Brodtkorb, P. A.; Lee, P.; McGibbon, R. T.; Feldbauer, R.; Lewis, S.; Tygier, S.; Sievert, S.; Vigna, S.; Peterson, S.; More, S.; Pudlik, T.; Oshima, T.; Pingel, T. J.; Robitaille, T. P.; Spura, T.; Jones, T. R.; Cera, T.; Leslie, T.; Zito, T.; Krauss, T.; Upadhyay, U.; Halchenko, Y. O.; Vázquez-Baeza, Y. SciPy 1.0: Fundamental Algorithms for Scientific Computing in Python. *Nat. Methods* **2020**, *17*, 261−272.
(78) Thiele, C. M.; Petzold, K.; Schleucher, J. EASY ROESY: Reliable Cross-Peak Integration in Adiabatic Symmetrized ROESY. *Chem. − Eur. J.* **2009**, *15*, 585−588.
(79) Eilers, P. H. C. A Perfect Smoother. *Anal. Chem.* **2003**, *75*, 3631−3636.
(80) Kneller, T. D.; Goddard, D. G. *SPARKY3*; University of California: San Francisco, 2004.
(81) Neuhaus, D. Nuclear Overhauser Effect. *Encyclopedia of Magnetic Resonance*; John Wiley & Sons, Ltd., 2011; pp 1−16.

https://doi.org/10.1021/acs.jmedchem.0c02036
J. Med. Chem. 2021, 64, 5365−5383